Chapter 11

Neutrino Scattering from Hadrons: Inelastic Scattering (I)

11.1 Introduction

The inelastic scattering processes of (anti)neutrinos from nucleons are relevant in the region starting from the neutrino energy corresponding to the threshold production of a single pion. For neutral current (NC) induced 1π production, this starts at $E^{\text{th}}_{\nu(\bar{\nu})} = 144.7$ MeV for ν_l reactions. In the case of charged current (CC) induced 1π production, the threshold energy is higher because of the massive leptons produced in the final state; it corresponds to $E_{\nu(\bar{\nu})} \geq$ 150.5 MeV (277.4 MeV) for ν_e (ν_μ) reactions. As the neutrino energy increases, inelastic processes of multiple pion production, viz., 2π, 3π, etc., and the production of strange mesons (K) and hyperons (Y) start; both of which are the most relevant inelastic processes in the region of a few GeV. These inelastic processes have been studied very extensively, both theoretically and experimentally, in various reactions induced by photons and electrons which probe the interaction of the electromagnetic vector currents with hadrons in the presence of other strongly interacting particles like mesons and hyperons. In weak processes induced by neutrinos and antineutrinos, the inelastic processes provide a unique opportunity to study the interaction of the weak vector as well as the axial vector currents with hadrons in the presence of strongly interacting particles like mesons and hyperons. Moreover, a study of these weak processes from nucleons and nuclei is of immense topical importance in the context of the present neutrino oscillation experiments being done with the accelerator and atmospheric neutrinos in the energy region of a few GeV. The specific reactions to be studied in the inelastic channels are the various processes induced by the charged and neutral weak currents of neutrinos and antineutrinos, given in Table 11.1.

The first four reactions in Table 11.1 are strangeness conserving $(\Delta S = 0)$ reactions and the last one is a strangeness changing $(\Delta S = 1)$ reaction. The generic Feynman diagrams describing these reactions are shown in Figures 11.1(a) and 11.1(b), where $\nu_l(\bar{\nu}_l)$ and $l^-(l^+)$

https://doi.org/10.1017/9781108489065.012 Published online by Cambridge University Press

Table 11.1 Charged and neutral current induced inelastic processes. N, N' represents protons and neutrons, $Y = \Lambda, \Sigma$ represents hyperons, $K = K^+, K^0$ represents kaons, $\bar{K} = K^-, \bar{K}^0$ represents antikaons, and $l = e, \mu, \tau$ represents leptons.

S. No.	CC induced $\nu(\bar{\nu})$ reactions	NC induced $\nu(\bar{\nu})$ reactions
1.	$\nu_l(\bar{\nu}_l) + N \longrightarrow l^-(l^+) + N' + \pi$	$\nu_l(\bar{\nu}_l) + N \longrightarrow \nu_l(\bar{\nu}_l) + N' + \pi$
2.	$\nu_l(\bar{\nu}_l) + N \longrightarrow l^-(l^+) + N' + n\pi$	$\nu_l(\bar{\nu}_l) + N \longrightarrow \nu_l(\bar{\nu}_l) + N' + n\pi$
3.	$\nu_l(\bar{\nu}_l) + N \longrightarrow l^-(l^+) + N' + \eta$	$\nu_l(\bar{\nu}_l) + N \longrightarrow \nu_l(\bar{\nu}_l) + N' + \eta$
4.	$\nu_l(\bar{\nu}_l) + N \longrightarrow l^-(l^+) + Y + K$	$\nu_l(\bar{\nu}_l) + N \longrightarrow \nu_l(\bar{\nu}_l) + Y + K$
5.	$\nu_l(\bar{\nu}_l) + N \longrightarrow l^-(l^+) + N' + K(\bar{K})$	$\nu_l(\bar{\nu}_l) + N \longrightarrow \nu_l(\bar{\nu}_l) + N' + K(\bar{K})$

are leptons interacting through the $W^{\pm}(Z)$ exchanges with the nucleon (N) producing the final nucleon (N') and hyperons (Y) and mesons like pions (π) and kaons (K). In Figure 11.1, the first vertex is the weak vertex (W) describing the weak interactions of leptons with $W^{\pm}(Z)$ bosons in the standard model (SM), while the second vertex is a mixed vertex (M) describing the weak interaction of nucleons in the SM and the strong interactions of the meson–baryon system described by a phenomenological Lagrangian consistent with the symmetries of strong interaction or effective Lagrangian motivated by the symmetries of quantum chromodynamics (QCD) like the chiral symmetry.

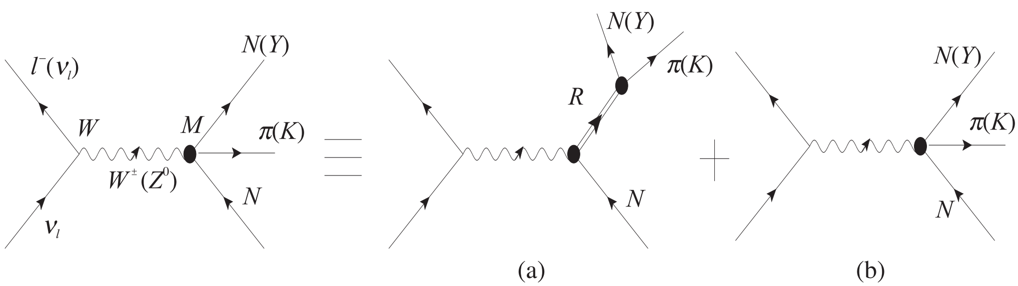

Figure 11.1 Generic Feynman diagrams representing the charged and neutral current induced inelastic processes given in Table 11.1.

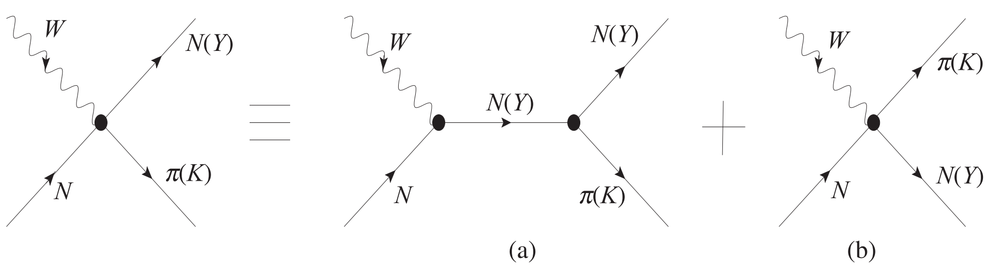

Figure 11.2 Generic Feynman diagrams representing the non-resonant background terms contributing to the inelastic processes.

It has been observed from the study of these inelastic reactions induced by photons and electrons in the case of electromagnetic interactions that the production processes are dominated

https://doi.org/10.1017/9781108489065.012 Published online by Cambridge University Press

by the excitation of nucleon resonances in the entire energy region as shown in Figure 11.1(a) except the region of very low energies corresponding to the threshold production of mesons where the non-resonant production of mesons shown in Figure 11.1(b) also makes important contribution. In Figure 11.1(a), R represents the excited resonance which decays into a nucleon and a pion or a hyperon and a strange meson in the case of $\Delta S = 0$ reactions; and to a nucleon and a strange meson in the case of $\Delta S = 1$ reactions. The diagrams showing the non-resonant direct production of mesons in Figure 11.1(b) receive contribution from two types of diagrams, that is, Born diagrams and contact diagrams, shown in Figure 11.2(a) and 11.2(b). The Born diagrams that are shown in Figure 11.2(a) contribute through the s, t, and u channel Feynman diagrams; while Figure 11.2(b) shows the contact diagram which appears in certain models of the effective Lagrangian for the meson–hadron interactions motivated by the chiral symmetry of QCD, and is responsible for the gauge invariance in the vector part of the hadronic current. These points are elaborated later in the text.

The nucleon resonances which are excited in the inelastic reactions are characterized by their mass, parity, spin, and isospin. They are represented by the symbol $R_{IJ}(M_R)$, where R is the name of the resonance given on the basis of the nucleon's orbital angular momentum, that is, $L = 0, 1, 2$. The resonances are named $S,\ P,\ D$, etc. M_R is the mass, while I and J specify their isospin and total angular momentum quantum numbers. The first resonance which is excited is called the Δ resonance, with positive parity, mass of 1232 MeV, isospin $3/2$, and spin $3/2$; it is therefore represented by the symbol $P_{33}(1232)$. The next excited resonance is called the Roper resonance which has negative parity, mass 1440 MeV, with spin $1/2$ and isospin $1/2$. The generic name given to a resonance with $I = 1/2$ is N^* resonance and to a resonance with $I = 3/2$ is Δ^* resonance. A list of resonances below the mass $M_R \leq 2.1$ GeV with spin $1/2$ and $3/2$ are given in Tables 11.2 and 11.3 along with the branching ratios of their dominant decays into various meson, nucleon, and hyperon channels.

Table 11.2 Properties of the spin $1/2$ resonances available in the Particle Data Group (PDG) [117] Breit–Wigner mass M_R, the total decay width Γ, isospin I, parity P, and the branching ratio of different meson–baryon systems like $N\pi$, $N\eta$, $K\Lambda$, and $K\Sigma$.

Resonance	Status	M_R (GeV)	Γ (GeV)	I	P	Branching ratios $N\pi$	$N\eta$	$K\Lambda$	$K\Sigma$
$P_{11}(1440)$	$****$	1.370 ± 0.01	0.175 ± 0.015	$1/2$	$+$	65%	$<1\%$	-	-
$S_{11}(1535)$	$****$	1.510 ± 0.01	0.130 ± 0.020	$1/2$	$-$	42%	42%	-	-
$S_{31}(1620)$	$****$	1.600 ± 0.01	0.120 ± 0.020	$3/2$	$-$	30%	-	-	-
$S_{11}(1650)$	$****$	1.655 ± 0.015	0.135 ± 0.035	$1/2$	$+$	60%	25%	10%	-
$P_{11}(1710)$	$****$	1.700 ± 0.02	0.120 ± 0.040	$1/2$	$+$	10%	30%	15%	$<1\%$
$P_{11}(1880)$	$***$	1.860 ± 0.04	0.230 ± 0.050	$1/2$	$+$	6%	30%	20%	17%
$S_{11}(1895)$	$****$	1.910 ± 0.02	0.110 ± 0.030	$1/2$	$-$	10%	25%	18%	13%
$S_{31}(1900)$	$****$	1.865 ± 0.035	0.240 ± 0.060	$3/2$	$-$	8%	-	-	-
$P_{31}(1910)$	$****$	1.860 ± 0.03	0.300 ± 0.100	$3/2$	$+$	20%	-	-	9%
$S_{31}(2150)$	$*$	2.140 ± 0.08	0.200 ± 0.080	$3/2$	$-$	8%	-	-	-

https://doi.org/10.1017/9781108489065.012 Published online by Cambridge University Press

Table 11.3 Properties of the spin $3/2$ resonances available in the PDG [117] with Breit–Wigner mass M_R, the total decay width Γ, isospin I, parity P, and the branching ratio of different meson–baryon systems like $N\pi$, $N\eta$, $K\Lambda$, and $K\Sigma$.

Resonance	Status	M_R (GeV)	Γ (GeV)	I	P	Branching ratios $N\pi$	$N\eta$	$K\Lambda$	$K\Sigma$
$P_{33}(1232)$	$****$	1.210 ± 0.001	0.100 ± 0.002	$3/2$	$+$	99.4%	-	-	-
$D_{13}(1520)$	$****$	1.510 ± 0.005	$0.110\pm^{0.010}_{0.005}$	$1/2$	$-$	60%	0.08%	-	-
$P_{33}(1600)$	$****$	1.510 ± 0.05	0.270 ± 0.07	$3/2$	$+$	16%	-	-	-
$D_{13}(1700)$	$***$	1.700 ± 0.05	0.200 ± 0.100	$1/2$	$-$	12%	12%	-	-
$D_{33}(1700)$	$****$	1.665 ± 0.025	0.250 ± 0.05	$3/2$	$-$	15%	-	-	-
$P_{13}(1720)$	$****$	1.675 ± 0.015	$0.250\pm^{0.100}_{0.150}$	$1/2$	$+$	11%	3%	4.5%	-
$D_{13}(1875)$	$***$	1.900 ± 0.05	0.160 ± 0.06	$1/2$	$-$	7%	$< 1\%$	0.2%	0.7%
$P_{13}(1900)$	$****$	1.920 ± 0.02	0.150 ± 0.05	$1/2$	$+$	10%	8%	11%	5%
$P_{33}(1920)$	$***$	1.900 ± 0.05	0.300 ± 0.1	$3/2$	$+$	12%	-	-	4%
$D_{33}(1940)$	$**$	1.950 ± 0.1	0.350 ± 0.15	$3/2$	$-$	4%	-	-	-
$D_{13}(2120)$	$***$	2.100 ± 0.05	0.280 ± 0.08	$1/2$	$-$	10%	-	-	-

In addition to nucleon resonances, there are meson and hyperon resonances which also contribute to the inelastic production of mesons and hyperons through t and u channels. Their contributions are traditionally included along with the contribution of the non-resonant part coming from the Born diagrams in s, t, and u channels. A list of low-lying meson and hyperon resonances are given in Tables 11.4 and 11.5; these resonances are generally included in many calculations of inelastic processes. They are calculated using an effective Lagrangian for the weak interaction vertex and an effective Lagrangian for the meson–baryon vertex. Since most of the calculations were done earlier for the single meson production dominated by the pion production at intermediate energies, an effective phenomenological Lagrangian for the pion nucleon interaction with pseudoscalar (ps) or pseudovector (pv) coupling is used. After the

Table 11.4 Properties of the meson (pion and kaon) resonances available in PDG [117] with Breit–Wigner mass M_R, the total decay width Γ, isospin I, spin J, and parity P.

Resonance	M_R (MeV)	Γ (MeV)	I	J	P
$\rho(770)$	775.26 ± 0.25	147.8 ± 0.9	1	1	$-$
$\omega(782)$	782.65 ± 0.12	8.49 ± 0.08	0	1	$-$
$K^*(892)$	891.66 ± 0.26	50.8 ± 0.9	$1/2$	1	$-$
$f_0(980)$	990 ± 20	$10 - 100$	0	0	$+$
$\phi(1020)$	1019.461 ± 0.016	4.249 ± 0.013	0	1	$-$
$h_1(1170)$	1170 ± 20	360 ± 40	0	1	$+$
$b_1(1235)$	1229.5 ± 3.2	142 ± 9	1	1	$+$
$K_1(1270)$	1272 ± 7	90 ± 20	$1/2$	1	$+$
$K_1(1400)$	1669 ± 7	$64\pm^{10}_{14}$	1	$3/2$	$-$

https://doi.org/10.1017/9781108489065.012 Published online by Cambridge University Press

Table 11.5 Properties of the spin $1/2$ and $3/2$ hyperon resonances available in PDG [117] with Breit–Wigner mass M_R, the total decay width Γ, isospin I, spin J, and parity P.

Resonance	Status	M_R (MeV)	Γ (MeV)	I	J	P
$\Lambda(1405)$	$****$	$1405.1\pm^{1.3}_{1.0}$	50.5 ± 2	0	1/2	−
$\Lambda(1520)$	$****$	1517 ± 4	$15\pm^{10}_{8}$	0	3/2	−
$\Lambda(1600)$	$***$	1544 ± 3	$112\pm^{12}_{2}$	0	1/2	+
$\Lambda(1690)$	$****$	1697 ± 6	65 ± 14	0	3/2	−
$\Lambda(1710)$	$*$	1713 ± 13	180 ± 40	0	1/2	+
$\Lambda(1800)$	$***$	$1800\pm^{50}_{80}$	300 ± 100	0	1/2	−
$\Lambda(2050)$	$*$	2056 ± 22	493 ± 60	0	3/2	−
$\Sigma(1385)$	$****$	1383.7 ± 1	36 ± 5	1	3/2	+
$\Sigma(1670)$	$****$	1669 ± 7	$64\pm^{10}_{14}$	1	3/2	−
$\Sigma(1730)$	$*$	1727 ± 27	276 ± 90	1	3/2	+
$\Sigma(1750)$	$***$	$1750\pm^{50}_{20}$	$90\pm^{70}_{30}$	1	1/2	−
$\Sigma(1940)$	$***$	$1940\pm^{10}_{40}$	$220\pm^{80}_{70}$	1	3/2	−

importance of the role of chiral symmetry in the study of strong interactions was realized, effective Lagrangians inspired by chiral symmetry have been used to describe meson–nucleon interactions. For this purpose, an effective Lagrangian based on chiral SU(2) symmetry has been used to describe the pion–nucleon interaction which is extended to chiral SU(3) symmetry to describe the kaon–nucleon interaction.

Early inelastic (anti)neutrino experiments were done on nuclear targets at CERN and later at ANL and BNL, the experiments were done on nucleons using hydrogen and deuterium targets [457, 458, 459]. In order to analyze the experimental results of the neutrino and antineutrino inelastic reactions on the nuclear targets, it is important to have a good understanding of the basic inelastic processes on nucleon targets. It is in this context that we give in this chapter, a theoretical formulation of the inelastic neutrino and antineutrino scattering processes on hadrons involving single meson production. There have been many approaches to calculate the single meson production from nucleons and nuclear targets induced by neutrinos and antineutrinos. Most of these methods have evolved from the treatment of photo- and electro- production of mesons from nucleons and nuclei which are induced by vector currents. In the case of weak production, there is an additional contribution from the axial vector current; the interference between the vector and axial vector contributions leads to parity violating observables in the single meson production.

Historically, weak pion production has been studied for a long time starting from 1962 [460, 461, 462, 463]. The early calculations were based on

(i) dynamical models with dispersion theory,

(ii) quark models with higher symmetry like SU(6),

(iii) phenomenological Lagrangians for the interaction of mesons with nucleons and higher resonances.

https://doi.org/10.1017/9781108489065.012 Published online by Cambridge University Press

These calculations have been comprehensively summarized by Adler [464] and Llewellyn Smith [294]; extensive calculations have also been done by Adler [464] in the dynamical model and in the quark model by Albright [465, 466] and Kim [467]. The calculations have been compared with the early experimental results from CERN [457]. After the results of the hydrogen and deuterium bubble chamber experiments from ANL [458] and BNL [459] and later experiments from CERN [468, 469, 470] were obtained, many new calculations were made using the phenomenological Lagrangians [471, 472, 473, 474, 475, 476, 477, 478, 479, 480] or the Lagrangians based on the chiral symmetry [481, 482, 483, 484, 485, 486, 487, 488, 489, 490, 491] or quark models [492].

As emphasized earlier in this section, the contributions from the resonance excitations and their subsequent decays play a more important role than the non-resonant diagrams. In the following sections, we outline a general formalism to calculate the resonance and non-resonant contribution to the single meson produced in the $\nu(\bar{\nu})$ reactions induced by the $\Delta S = 0$ and $\Delta S = 1$ weak charge current (CC) and also the $\Delta S = 0$ neutral current (NC).

11.2 Inelastic Scattering through CC Excitation of Resonances

Tables 11.2 and 11.3 presented the properties of spin $1/2$ and $3/2$ resonances. There also exist, in nature, many baryon resonances with higher spins like spin $5/2, 7/2, 9/2$, etc. For example, $D_{15}(1675)$ is spin 5/2 resonance with a $***\,**$ rating, which means that experimentally $D_{15}(1675)$ is a well-studied resonance but theoretically, the physics of such higher spin resonances like $D_{15}(1675)$ is very complicated and beyond the scope of this book. In Sections 11.2.1 and 11.2.2, we present the formalism to study charged current induced resonance excitations with spin $1/2$ and $3/2$.

11.2.1 CC excitation of spin $1/2$ resonances

Excitation of spin $1/2$ and isospin $1/2$ resonances

The basic (anti)neutrino induced spin $1/2$ resonance excitations on the nucleon target are the following:

$$\nu_l/\bar{\nu}_l\ (k) + N(p) \longrightarrow l^-/l^+\ (k') + R_{1/2}(p_R). \tag{11.1}$$

The invariant matrix element for the process, given in Eq. (11.1) and depicted in Figure 11.3, is written as

$$\mathcal{M} = \frac{G_F}{\sqrt{2}} \cos\theta_C\, l_\mu\, J^{\mu CC}_{\frac{1}{2}}, \tag{11.2}$$

where G_F is the Fermi coupling constant and θ_C is the Cabibbo mixing angle. The leptonic current l^μ is the same as in the case of quasielastic scattering; however, for the sake of completeness, the expression is given as:

https://doi.org/10.1017/9781108489065.012 Published online by Cambridge University Press

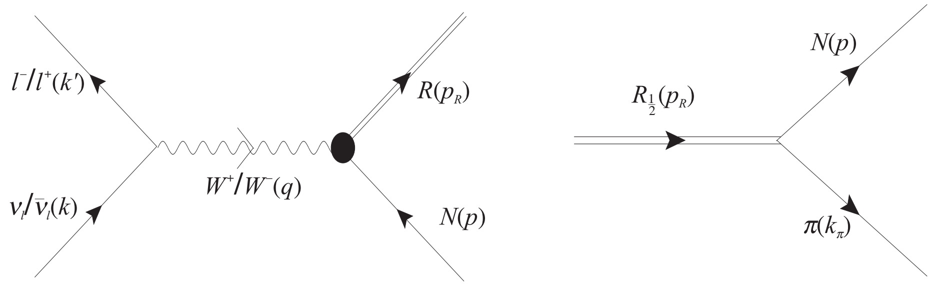

Figure 11.3 Feynman diagram for the charged current induced spin $1/2$ and $3/2$ resonance production (left panel) and for the decay of the resonance into a nucleon and a pion (right panel). The quantities in the parentheses represent the momenta of the corresponding particles.

$$l_\mu = \bar{u}(k')\gamma_\mu(1 \mp \gamma_5)u(k). \tag{11.3}$$

$(+)-$ represents the (anti)neutrino induced processes. The hadronic current for the spin $\frac{1}{2}$ resonance is given by

$$J^{\mu CC}_{\frac{1}{2}} = \bar{u}(p_R)\Gamma^\mu_{\frac{1}{2}} u(p), \tag{11.4}$$

where $u(p)$ and $\bar{u}(p_R)$, respectively, are the Dirac spinor and adjoint Dirac spinor for the initial nucleon and the final spin $1/2$ resonance. $\Gamma^\mu_{\frac{1}{2}}$ is the vertex function. For a positive parity resonance, $\Gamma^\mu_{\frac{1}{2}}$ is given by

$$\Gamma^\mu_{\frac{1}{2}^+} = V^\mu_{\frac{1}{2}} - A^\mu_{\frac{1}{2}}, \tag{11.5}$$

while for a negative parity resonance, $\Gamma^\mu_{\frac{1}{2}}$ is given by

$$\Gamma^\mu_{\frac{1}{2}^-} = \left[V^\mu_{\frac{1}{2}} - A^\mu_{\frac{1}{2}} \right] \gamma_5, \tag{11.6}$$

where $V^\mu_{\frac{1}{2}}$ represents the vector current and $A^\mu_{\frac{1}{2}}$ represents the axial vector current.

The vector and axial vector currents are parameterized in terms of the vector and axial vector $N - R_{1/2}$ transition form factors, respectively, as,

$$V^\mu_{\frac{1}{2}} = \frac{F_1^{CC}(Q^2)}{(2M)^2}\left(Q^2\gamma^\mu + \not{q}q^\mu \right) + \frac{F_2^{CC}(Q^2)}{2M} i\sigma^{\mu\alpha}q_\alpha \tag{11.7}$$

$$A^\mu_{\frac{1}{2}} = \left[F_A^{CC}(Q^2)\gamma^\mu + \frac{F_P^{CC}(Q^2)}{M} q^\mu \right] \gamma_5, \tag{11.8}$$

https://doi.org/10.1017/9781108489065.012 Published online by Cambridge University Press

where $Q^2 = -q^2 = -(k-k')^2$. $F_{1,2}^{CC}(Q^2)$ represents the weak vector form factors for the $N - R_{1/2}$ transitions while $F_{A,P}^{CC}(Q^2)$ represents the axial vector form factors. In the following sections, we discuss how these vector and axial vector form factors for the charged current resonance production are determined.

(i) Vector form factors

The weak vector form factors $F_{1,2}^{CC}(Q^2)$ are related to the electromagnetic $N - R_{1/2}$ transition form factors for the spin $1/2$ resonances, viz., $F_{1,2}^{R^+}(Q^2)$ and $F_{1,2}^{R^0}(Q^2)$, by the isospin symmetry and are expressed as:

$$F_i^{CC}(Q^2) = F_i^{R^+}(Q^2) - F_i^{R^0}(Q^2), \qquad i = 1,2. \tag{11.9}$$

The hypothesis of the conserved vector current (CVC) states that the components of the weak charged vector currents and isovector electromagnetic current form an isotriplet in the isospin space, that is, the charged current vector form factors are related to the electromagnetic form factors by isospin symmetry. The isovector part of the weak current $\mathcal{J}_\mu^i$ can be written as

$$\mathcal{J}_\mu^i = (\mathcal{J}_\mu^1, \mathcal{J}_\mu^2, \mathcal{J}_\mu^3) = \mathcal{V}_\mu^i - \mathcal{A}_\mu^i, \qquad i = 1-3 \tag{11.10}$$

where

$$\mathcal{V}_\mu^i = (\mathcal{V}_\mu^1, \mathcal{V}_\mu^2, \mathcal{V}_\mu^3) = V_\mu \frac{\tau^i}{2}, \tag{11.11}$$

$$\mathcal{A}_\mu^i = (\mathcal{A}_\mu^1, \mathcal{A}_\mu^2, \mathcal{A}_\mu^3) = A_\mu \frac{\tau^i}{2}, \tag{11.12}$$

with V_μ and A_μ as defined in Eqs. (11.7) and (11.8), respectively. τ_is are the Pauli spin matrices.

Let us start with the electromagnetic current which is given by the following expression

$$J_\mu^{EM} = \frac{1}{2}\mathcal{V}_\mu^I + \mathcal{V}_\mu^3, \tag{11.13}$$

where $\mathcal{V}_\mu^3$ represents the third component of the isovector vector current ($|I, I_3\rangle = |1,0\rangle$) and $\mathcal{V}_\mu^I$ is the isoscalar current ($|I, I_3\rangle = |0,0\rangle$).

In the case of the isospin $1/2$ resonances, both isoscalar and isovector components of the electromagnetic current given in Eq. (11.13) contribute. The isoscalar part of the electromagnetic current, $\mathcal{V}_\mu^I$ is defined as

$$\mathcal{V}_\mu^I = V_\mu^I I_{2\times 2}, \tag{11.14}$$

where $I_{2\times 2}$ represents the 2×2 identity matrix.

https://doi.org/10.1017/9781108489065.012 Published online by Cambridge University Press

In terms of the form factors, the matrix element for the electromagnetic current for the transition $N - R_{1/2}$ is given as:

$$\langle R^+_{1/2}| J^{EM}_\mu |p\rangle = \bar{u}(p_R)\left[\frac{F_1^{R^+_{1/2}}(Q^2)}{(2M)^2}\left(Q^2\gamma^\mu + q^\mu \not{q}\right) + \frac{F_2^{R^+_{1/2}}(Q^2)}{2M} i\sigma^{\mu\alpha}q_\alpha\right]\Gamma u(p) = V_\mu^{R^+_{1/2}}, \tag{11.15}$$

$$\langle R^0_{1/2}| J^{EM}_\mu |n\rangle = \bar{u}(p_R)\left[\frac{F_1^{R^0_{1/2}}(Q^2)}{(2M)^2}\left(Q^2\gamma^\mu + q^\mu \not{q}\right) + \frac{F_2^{R^0_{1/2}}(Q^2)}{2M} i\sigma^{\mu\alpha}q_\alpha\right]\Gamma u(p) = V_\mu^{R^0_{1/2}}, \tag{11.16}$$

where $\Gamma = 1$ (γ_5) for the positive (negative) parity resonances.

The transition matrix element for the process $\gamma N \to R_{1/2}$ is written as

$$\langle R_{1/2}| \mathcal{J}^{EM}_\mu |N\rangle \;=\; \langle R_{1/2}| \mathcal{V}^3_\mu + \frac{1}{2}\mathcal{V}^I_\mu |N\rangle\,, \tag{11.17}$$

where $|N\rangle = \begin{pmatrix} p \\ n \end{pmatrix}$ represents the nucleon field and $|R_{1/2}\rangle = \begin{pmatrix} R^+_{1/2} \\ R^0_{1/2} \end{pmatrix}$ represents the spin 1/2 resonance field. Using Eqs. (11.11) and (11.14) in Eq.(11.17), we obtain

$$\begin{aligned}
\langle R_{1/2}| \mathcal{J}^{EM}_\mu |N\rangle &= \langle R_{1/2}| V_\mu \frac{\tau_3}{2} + V^I_\mu \frac{I_{2\times 2}}{2} |N\rangle\,, \\
&= \begin{pmatrix} \bar{R}^+_{1/2} & \bar{R}^0_{1/2} \end{pmatrix} \begin{pmatrix} \frac{V_\mu + V^I_\mu}{2} & 0 \\ 0 & \frac{-V_\mu + V^I_\mu}{2} \end{pmatrix} \begin{pmatrix} p \\ n \end{pmatrix}, \\
&= \bar{R}^+_{1/2}\left(\frac{V_\mu + V^I_\mu}{2}\right) p + \bar{R}^0_{1/2}\left(\frac{-V_\mu + V^I_\mu}{2}\right) n.
\end{aligned} \tag{11.18}$$

Comparing Eqs. (11.15) and (11.16) with the first and second terms of Eq. (11.18), we obtain

$$V_\mu^{R^+_{1/2}} = (V_\mu + V^I_\mu)/2, \tag{11.19}$$

$$V_\mu^{R^0_{1/2}} = (-V_\mu + V^I_\mu)/2. \tag{11.20}$$

From Eqs. (11.19) and (11.20), V_μ and V^I_μ are obtained as

$$V_\mu = V_\mu^{R^+_{1/2}} - V_\mu^{R^0_{1/2}}, \tag{11.21}$$

$$V^I_\mu = V_\mu^{R^+_{1/2}} + V_\mu^{R^0_{1/2}}. \tag{11.22}$$

The vector current for the charged current process (given in Eq. (11.7)) is written as

$$V^{CC}_\mu = \mathcal{V}^1_\mu + i\mathcal{V}^2_\mu, \tag{11.23}$$

https://doi.org/10.1017/9781108489065.012 Published online by Cambridge University Press

where $\mathcal{V}^1_\mu$ and $\mathcal{V}^2_\mu$ are the components of the isovector currents.

Now, writing the transition matrix element for the vector part of the charged current process, $nW^+ \rightarrow R^+_{1/2}$, we have

$$\begin{aligned}
\langle R^+_{1/2}| V^{CC}_\mu |n\rangle &= \langle R^+_{1/2}| \mathcal{V}^1_\mu + i\mathcal{V}^2_\mu |n\rangle\,, \\
&= \langle R^+_{1/2}| V_\mu \tau_+ |n\rangle\,, \\
&= V_\mu, \\
&= V_\mu^{R^{\frac{1}{2}}_{+}} - V_\mu^{R^{\frac{1}{2}}_{0}}
\end{aligned} \tag{11.24}$$

where $\tau_+ = \frac{1}{2}(\tau_1 + i\tau_2)$. Thus, Eqs. (11.21), (11.22), and (11.24) relates the electromagnetic and weak vector form factors with each other and the relation is given in Eq. (11.9).

It must be noted that the relation between the electromagnetic and weak vector form factors, as obtained here, depends only on the isospin of the resonance considered. Therefore, the weak vector form factors for the spin $3/2$ and isospin $1/2$ resonances are related to the electromagnetic form factors in a similar manner as obtained in Eq. (11.9) for the spin $1/2$ and isospin $1/2$ resonances.

(ii) Electromagnetic form factors and the helicity amplitude

The electromagnetic form factors $F_i^{R^+,R^0}(Q^2)$, $(i = 1,2)$ are derived from the helicity amplitudes extracted from real and/or virtual photon scattering experiments. In order to determine the helicity amplitudes $A_{1/2}$ and $S_{1/2}$, assume the interaction of a nucleon with a virtual/real photon to produce a spin $1/2$ resonance. The helicity amplitudes for the process $\gamma N \rightarrow R_{1/2}$ are expressed in terms of the polarization of the photon and the spins of the incoming nucleon and the outgoing spin $1/2$ resonance. They are depicted in Figure 11.4, where we have fixed the spin of the resonance in the positive Z direction, that is, $J^R_z = +1/2$. It must be noted that it is our choice to fix $J^R_z = +1/2$; one may obtain the expressions for the helicity amplitudes by fixing $J^R_z = -1/2$. The expressions for $A_{1/2}$ and $S_{1/2}$ are defined as [483]:

$$A^N_{1/2} = \sqrt{\frac{2\pi\alpha}{K_R}}\, \langle R, J^R_z = +1/2|\, \epsilon^+_\mu \Gamma^\mu \,|N, J^N_z = -1/2\rangle\, \zeta, \tag{11.25}$$

$$S^N_{1/2} = -\sqrt{\frac{2\pi\alpha}{K_R}}\frac{|\vec{q}|}{\sqrt{Q^2}}\, \langle R, J^R_z = +1/2|\, \epsilon^0_\mu \Gamma^\mu \,|N, J^N_z = +1/2\rangle\, \zeta, \tag{11.26}$$

where $K_R = (M_R^2 - M^2)/2M_R$ is the momentum of the real photon measured in the resonance rest frame and $|\vec{q}|$ is the momentum of the virtual photon measured in the laboratory frame given as

$$|\vec{q}| = \sqrt{\frac{(M_R^2 - M^2 - Q^2)^2}{(2M_R)^2} + Q^2}. \tag{11.27}$$

Γ^μ is the electromagnetic transition current for the positive and negative parity resonances, defined as $\Gamma^\mu = V^\mu$. The expressions for V^μ is given in Eq. (11.7). $\zeta = e^{i\phi}$, where ϕ is

https://doi.org/10.1017/9781108489065.012 Published online by Cambridge University Press

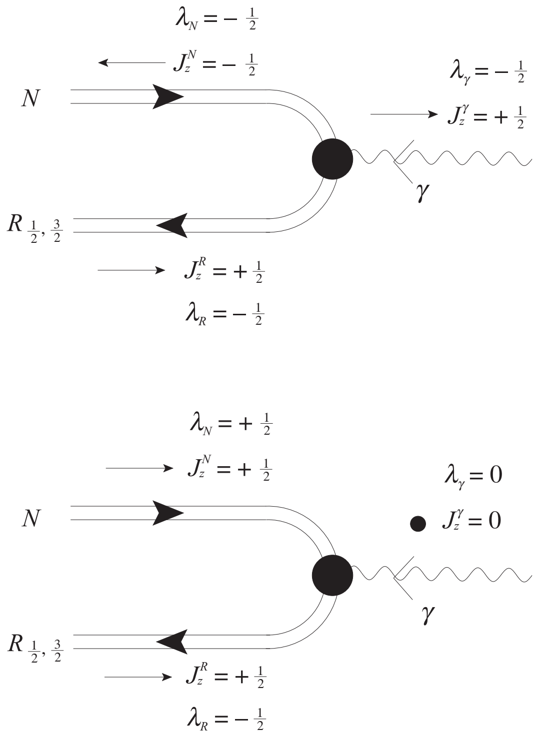

Figure 11.4 Diagrammatic representation of the helicity amplitudes, $A_{1/2}$ (top) and $S_{1/2}$ (bottom) for spin $1/2$ and $3/2$ resonances.

the phase factor which relates how the amplitude of the resonances and the nucleons are added. Generally, ϕ is taken to be 0 but this is not a rule of thumb. ϵ_μ represents the photon polarization vector. The transverse polarized photon vector, $\epsilon_\mu^\pm$ is given as

$$\epsilon_\mu^\pm = \mp\frac{1}{\sqrt{2}}(0, 1, \pm i, 0). \tag{11.28}$$

For the longitudinal polarization of the photon, ϵ_μ^0 is given as

$$\epsilon_\mu^0 = \frac{1}{\sqrt{Q^2}}(|\vec{q}|, 0, 0, q^0), q^0 = |\vec{q}|. \tag{11.29}$$

From Eqs. (11.25), (11.26), (11.28), and (11.29), one may observe that for the spin $1/2$ resonances, $A_{1/2}$ represents the interaction of the transverse polarized photons with the $NR_{1/2}$ vertex. $S_{1/2}$ represents the interaction of the longitudinally polarized photons with the $NR_{1/2}$ vertex.

Using Eqs. (11.25)–(11.29), one can calculate the explicit relations between the form factors $F_i^{R^+,R^0}(Q^2)$ and the helicity amplitudes $A_{\frac{1}{2}}^{p,n}(Q^2)$ and $S_{\frac{1}{2}}^{p,n}(Q^2)$. These are given by [483]:

https://doi.org/10.1017/9781108489065.012 Published online by Cambridge University Press

$$
\begin{aligned}
A^{p,n}_{\frac{1}{2}} &= \sqrt{\frac{2\pi\alpha}{M}\frac{(M_R \mp M)^2+Q^2}{M_R^2-M^2}}\left[\frac{Q^2}{4M^2}F_1^{R^+,R^0}(Q^2)+\frac{M_R\pm M}{2M}F_2^{R^+,R^0}(Q^2)\right],\\
S^{p,n}_{\frac{1}{2}} &= \mp\sqrt{\frac{\pi\alpha}{M}\frac{(M\pm M_R)^2+Q^2}{M_R^2-M^2}\frac{(M_R\mp M)^2+Q^2}{4M_RM}}\\
&\quad \left[\frac{M_R\pm M}{2M}F_1^{R^+,R^0}(Q^2)-F_2^{R^+,R^0}(Q^2)\right],
\end{aligned}
\tag{11.30}
$$

where upper (lower) sign represents the positive (negative) parity resonance state and M_R is the mass of the corresponding resonance.

The Q^2 dependence of the helicity amplitudes is parameterized by the MAID group as [493]

$$
\mathcal{A}_\alpha(Q^2) = \mathcal{A}_\alpha(0)(1+a_1Q^2+a_2Q^4+a_3Q^6+a_4Q^8)\,e^{-b_1Q^2},
\tag{11.31}
$$

where $\mathcal{A}_\alpha(Q^2)$ is the helicity amplitude, viz., $A_{\frac{1}{2}}(Q^2)$ and $S_{\frac{1}{2}}(Q^2)$. Parameters $\mathcal{A}_\alpha(0)$ are generally determined by a fit to the photoproduction data of the corresponding resonance, while the parameters a_i $(i=1-4)$ and b_1 for each amplitude are obtained from the electroproduction data available at different Q^2. Once the parameters a_i and b_1 are fixed for $A_{\frac{1}{2}}(Q^2)$ and $S_{\frac{1}{2}}(Q^2)$ amplitudes, one gets the form factors $F_{1,2}^{R^+,R^0}(Q^2)$. Not all the resonances quoted in Table 11.2 are well understood. Hence, the MAID group has parameterized the values of these parameters for the resonances which are experimentally studied in the photo- and electro- productions. The values of these parameters are presented in Tables 11.6 and 11.7 for proton and neutron targets, respectively. It must be noted that for the isospin $3/2$ resonances, irrespective of the spin of the resonance, the different parameters for $A_{1/2}$ and $S_{1/2}$ given in Eq. (11.31) have the same values for the proton and neutron targets.

Table 11.6 MAID parameterization [493] of the transition form factors for the spin $1/2$ resonance on a proton target. $\mathcal{A}_\alpha(0)$ is given in units of $10^{-3}\,\mathrm{GeV}^{-\frac{1}{2}}$ and the coefficients a_1, a_2, a_4, b_1 in units of GeV^{-2}, GeV^{-4}, GeV^{-8}, GeV^{-2}, respectively. For all fits, $a_3 = 0$. For $S_{11}(1535)$, $S_{31}(1620)$, and $S_{11}(1650)$, resonance a_2 and a_4 are taken to be 0.

N^*	Amplitude	$\mathcal{A}_\alpha(0)$	a_1	a_2	a_4	b_1
$P_{11}(1440)$	$A_{\frac{1}{2}}$	-61.4	0.871	-3.516	-0.158	1.36
	$S_{\frac{1}{2}}$	4.2	40.0	0	1.50	1.75
$S_{11}(1535)$	$A_{\frac{1}{2}}$	66.4	1.608	0	0	0.70
	$S_{\frac{1}{2}}$	-2.0	23.9	0	0	0.81
$S_{31}(1620)$	$A_{\frac{1}{2}}$	65.6	1.86	0	0	2.50
	$S_{\frac{1}{2}}$	16.2	2.83	0	0	2.00
$S_{11}(1650)$	$A_{\frac{1}{2}}$	33.3	1.45	0	0	0.62
	$S_{\frac{1}{2}}$	-3.5	2.88	0	0	0.76

https://doi.org/10.1017/9781108489065.012 Published online by Cambridge University Press

Table 11.7 MAID parameterization [493] for a neutron target ($a_{2,3,4} = 0$) for spin $1/2$ resonances.

N^*	Amplitude	$\mathcal{A}_\alpha(0)$	a_1	b_1
$P_{11}(1440)$	$A_{\frac{1}{2}}$	54.1	0.95	1.77
	$S_{\frac{1}{2}}$	−41.5	2.98	1.55
$S_{11}(1535)$	$A_{\frac{1}{2}}$	−50.7	4.75	1.69
	$S_{\frac{1}{2}}$	28.5	0.36	1.55
$S_{11}(1650)$	$A_{\frac{1}{2}}$	9.3	0.13	1.55
	$S_{\frac{1}{2}}$	10.	−0.5	1.55

(iii) Axial vector form factors

The axial vector current consists of two form factors, viz., $F_A^{CC}(Q^2)$ and $F_P^{CC}(Q^2)$. Experimentally, information regarding the axial vector form factors is scarce. As in the case of quasielastic scattering, the pseudoscalar form factor $F_P^{CC}(Q^2)$ is related to $F_A^{CC}(Q^2)$ by the assumption of partially conserved axial vector current (PCAC) and the pion pole dominance. The value of $F_A^{CC}(0)$ is determined by the off-diagonal Goldberger–Treiman relation. We have seen earlier in Chapters 6 and 10 that the axial vector current is conserved only in the chiral limit, that is, $m_\pi \to 0$.

The divergence of the axial vector current in Eq. (11.8) yields

$$\begin{aligned} \partial_\mu A^\mu_{1/2\pm} &= -iq_\mu A^\mu_{1/2\pm} = i\bar{u}(p_R)\left[F_A^{CC}\not{q}\gamma_5 + \frac{F_P^{CC}}{M}q^2\gamma_5\right]\Gamma u(p), \\ &= i\bar{u}(p_R)\left[F_A^{CC}(M_R \pm M)\gamma_5 + \frac{F_P^{CC}}{M}q^2\gamma_5\right]\Gamma u(p), \end{aligned} \tag{11.32}$$

where $\Gamma = 1$ (γ_5) for positive (negative) parity resonances. According to the PCAC hypothesis, this expression must be proportional to the square of the pion mass. The second term in Eq. (11.32) with the pseudoscalar form factor has a pion pole.

The pion pole contribution can be obtained by applying the same procedure as we have done for obtaining the Goldberger–Treiman relation in the case of nucleons in Chapter 6. Consider that a nucleon transforms to a spin $1/2$ resonance by emitting a pion and this pion then decays to a $l^-\bar{\nu}_l$ pair as shown in Figure 11.5. The matrix element for the axial vector current is written in terms of

(i) the strong $NR_{1/2}\pi$ vertex,

(ii) the pion propagator, and

(iii) the current at the leptonic vertex ($\pi \to l^-\bar{\nu}_l$),

as:

$$A^\mu = (A^{N\to R_{1/2}\pi}) \times \left(\frac{i}{k_\pi^2 - m_\pi^2}\right) \times (-i\sqrt{2}f_\pi k_\pi^\mu), \tag{11.33}$$

https://doi.org/10.1017/9781108489065.012 Published online by Cambridge University Press

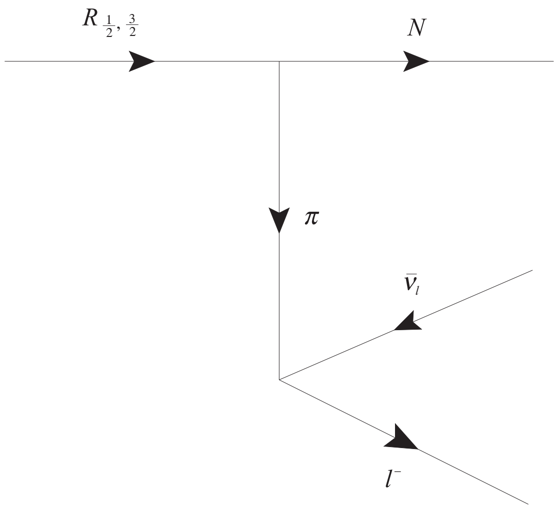

Figure 11.5 Feynman diagram of the process $R_{\frac{1}{2},\frac{3}{2}} \to Nl^-\bar{\nu}_l$ through pion decay.

where k_π is the momentum of the pion and f_π is the pion decay constant. The current at the $NR_{1/2}\pi$ vertex is determined by the pseudovector Lagrangian $\mathcal{L}_{NR_{1/2}\pi}$, given as

$$\mathcal{L}_{NR_{1/2}\pi} = C_{\text{iso}}\, \frac{f_{NR_{1/2}\pi}}{m_\pi} \bar{\psi}_R \Gamma^\mu \partial_\mu \vec{\phi} \cdot \vec{\tau}\, \psi, \tag{11.34}$$

where C_{iso} is the isospin factor. For $N \longrightarrow R^+_{1/2}$ transition, the value of C_{iso} is

$$C_{\text{iso}} = \sqrt{2}. \tag{11.35}$$

$f_{NR_{1/2}\pi}$ is the coupling of the $NR_{1/2}\pi$ vertex which is obtained using the partial decay width of $R_{1/2} \to N\pi$. This coupling is later discussed in the text. $\Gamma^\mu = \gamma^\mu\gamma_5$ (γ^μ) stands for the positive (negative) parity resonances and ϕ represents the triplet of the pion field. Using the Lagrangian given in Eq. (11.34), the matrix element for the axial vector current for the $N(p) \to R_{1/2}(p_R) + \pi(k_\pi)$ vertex is written as

$$A^{N\to R_{1/2}\pi} = -i\bar{u}(p_R)\left(C_{\text{iso}}\frac{f}{m_\pi}\Gamma_\mu \partial^\mu \phi\right) u(p). \tag{11.36}$$

Using Eq. (11.36) in Eq. (11.33), the matrix element for the pion pole contribution is obtained as

$$\begin{aligned} A^\mu &= -iC_{\text{iso}}\, \bar{u}(p_R)\frac{f_{NR_{1/2}\pi}}{m_\pi}\Gamma_\alpha \partial^\alpha \phi u(p)\, \frac{\sqrt{2} f_\pi k_\pi^\mu}{k_\pi^2 - m_\pi^2} \\ &= -iC_{\text{iso}}\, \bar{u}(p_R)\frac{f_{NR_{1/2}\pi}}{m_\pi}\gamma_\alpha(-ik_\pi^\alpha)\Gamma u(p)\, \frac{\sqrt{2} f_\pi k_\pi^\mu}{k_\pi^2 - m_\pi^2} \end{aligned}$$

https://doi.org/10.1017/9781108489065.012 Published online by Cambridge University Press

$$= \quad -C_{\rm iso}\, \bar{u}(p_R)\frac{f_{NR_{1/2}\pi}}{m_\pi}(M_R \pm M)\Gamma u(p)\, \frac{\sqrt{2} f_\pi k_\pi^\mu}{k_\pi^2 - m_\pi^2}. \tag{11.37}$$

From the definitions of q and k_π, it must be observed that the two represent the same quantity, that is, $q^\mu = p_R^\mu - p^\mu = k_\pi^\mu$. Comparing Eq. (11.37) with the second part of Eq. (11.8), the pseudoscalar form factor F_P^{CC} is obtained as

$$F_P^{CC} = -C_{\rm iso}\,\sqrt{2} f_\pi \frac{f_{NR_{1/2}\pi}}{m_\pi}\frac{(M_R \pm M)M}{Q^2 + m_\pi^2}. \tag{11.38}$$

Using the expression of F_P^{CC} as obtained here, Eq. (11.32) may be rewritten as

$$\partial_\mu A^\mu_{1/2\pm} = i\bar{u}(p_R)\left[F_A^{CC}(M_R \pm M)\gamma_5 - C_{\rm iso}\,\sqrt{2} f_\pi \frac{f_{NR_{1/2}\pi}}{m_\pi}\frac{(M_R \pm M)}{Q^2 + m_\pi^2} q^2\gamma_5\right]\Gamma u(p). \tag{11.39}$$

In the chiral limit, $m_\pi \to 0$, this expression reduces to

$$\partial_\mu A^\mu_{1/2\pm} = i\bar{u}(p_R)\left[F_A^{CC}(M_R \pm M)\gamma_5 + C_{\rm iso}\,\sqrt{2} f_\pi \frac{f_{NR_{1/2}\pi}}{m_\pi}(M_R \pm M)\gamma_5\right]\Gamma u(p). \tag{11.40}$$

The chiral limit demands $\partial_\mu A^\mu_{1/2\pm} = 0$, which is possible only if

$$F_A^{CC}(M_R \pm M) \quad = \quad -C_{\rm iso}\,\sqrt{2} f_\pi \frac{f_{NR_{1/2}\pi}}{m_\pi}(M_R \pm M) \tag{11.41}$$

which yields the generalized Goldberger–Treiman relation as

$$F_A^{CC} = -C_{\rm iso}\,\sqrt{2} f_\pi \frac{f_{NR_{1/2}\pi}}{m_\pi}. \tag{11.42}$$

This expression gives the values of $F_A(0)$ for the isospin $I = 1/2$ resonances using the value of $C_{\rm iso}$ given in Eq. (11.35) as:

$$F_A^{CC}(0)\Big|_{I=1/2} \quad = \quad -2 f_\pi \frac{f_{NR_{1/2}\pi}}{m_\pi}. \tag{11.43}$$

There is not much information about the Q^2 dependence of the axial vector form factor F_A^{CC} (Q^2), therefore, a dipole parameterization of $F_A^{CC}(Q^2)$, in analogy with the quasielastic scattering, is assumed:

$$F_A^{CC}(Q^2) = F_A^{CC}(0)\left(1 + \frac{Q^2}{M_A^2}\right)^{-2} \tag{11.44}$$

with $M_A \sim 1$ GeV.

https://doi.org/10.1017/9781108489065.012 Published online by Cambridge University Press

Using Eq. (11.42) in Eq. (11.38), the pseudoscalar form factor $F_P^{CC}(Q^2)$ is obtained in terms of $F_A^{CC}(Q^2)$ as

$$F_P^{CC}(Q^2) = \frac{(MM_R \pm M^2)}{m_\pi^2 + Q^2} F_A^{CC}(Q^2), \tag{11.45}$$

where the $+(-)$ sign is for positive (negative) parity resonances. The Q^2 dependence of the form factors, thus, obtained are shown in Figures 11.6 and 11.7, respectively for $S_{11}(1650)$ and $P_{11}(1440)$ resonances.

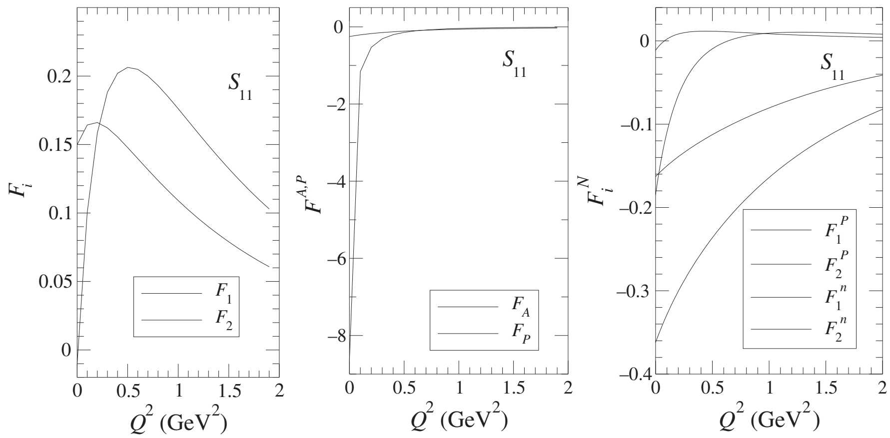

Figure 11.6 Q^2 dependence of different form factors of $S_{11}(1650)$ resonance. In the left panel, the form of isovector form factors F_1^{CC} and F_2^{CC} are shown in the form in which they are given in Eq. (11.9). In the middle panel, we have shown the axial form factors $F_{A,P}$ where for F_A, we took the dipole form and F_P is obtained from Eq. (11.45). In the right panel, we have shown the explicit dependence of $F_i^{R^+,R^0}$, $i = 1,2$ which may be obtained from the helicity amplitudes as given in Eq. (11.30).

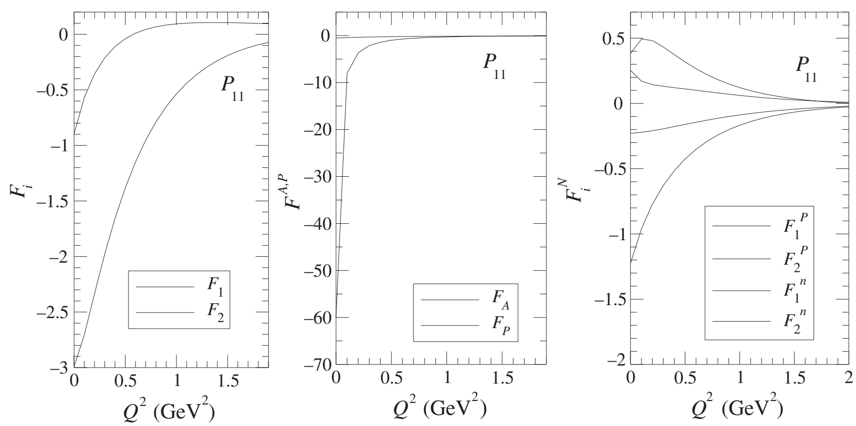

Figure 11.7 Q^2 dependence of different form factors of $P_{11}(1440)$ resonance. The lines have the same meaning as in Figure 11.6.

https://doi.org/10.1017/9781108489065.012 Published online by Cambridge University Press

Excitation of spin $1/2$ and isospin $3/2$ R_{13} resonances

(i) Vector form factors

In this section, we discuss how the weak vector form factors are related to electromagnetic ones when the transition of N to isospin $3/2$ and spin $1/2$ resonances is taken into account. The vector and axial vector currents, which constitute the electroweak current given in Eq. (11.10), for the isospin $1/2 \to 3/2$ transition are defined using transition operator $T^\dagger$ as

$$\mathcal{V}_\mu = -\sqrt{\frac{3}{2}} V_\mu T^\dagger, \tag{11.46}$$

$$\mathcal{A}_\mu = -\sqrt{\frac{3}{2}} A_\mu T^\dagger. \tag{11.47}$$

Let us start with the isospin $1/2 \to 3/2$ transition operator $T^\dagger$, which is a collection of three 4×2 matrices that connects the nucleon field with the corresponding isospin $3/2$ resonance field. Each 4×2 matrix is basically a Clebsch–Gordan array. This transition operator $T^\dagger$ is defined in terms of the matrix elements of the components of T_λ, where λ is defined using a spherical basis. The normalization of the transition operator $T^\dagger_\lambda$ is given as:

$$\langle\frac{3}{2}, M|T^\dagger_\lambda|\frac{1}{2}, m\rangle = \left(1, \frac{1}{2}, \frac{3}{2}|\lambda, m, M\right). \tag{11.48}$$

The right-hand side of Eq. (11.48) represents the Clebsch–Gordan coefficients for the process $N(|I, I_3 = 1/2, \pm 1/2\rangle) + \gamma(|I, I_3 = 1, 0\rangle) \to R_{1/2}(|I, I_3 = 3/2, \pm 3/2 \pm 1/2\rangle)$. The three 4×2 matrices for the $\langle\frac{3}{2}, M|T^\dagger_\lambda|\frac{1}{2}, m\rangle$, where $\lambda = -1, 0, +1$, are given as

$$\begin{aligned}
T^\dagger_{-1} &= \begin{pmatrix} (1,\frac{1}{2},\frac{3}{2}|-1,+\frac{1}{2},+\frac{3}{2}) & (1,\frac{1}{2},\frac{3}{2}|-1,-\frac{1}{2},+\frac{3}{2}) \\ (1,\frac{1}{2},\frac{3}{2}|-1,+\frac{1}{2},+\frac{1}{2}) & (1,\frac{1}{2},\frac{3}{2}|-1,-\frac{1}{2},+\frac{1}{2}) \\ (1,\frac{1}{2},\frac{3}{2}|-1,+\frac{1}{2},-\frac{1}{2}) & (1,\frac{1}{2},\frac{3}{2}|-1,-\frac{1}{2},-\frac{1}{2}) \\ (1,\frac{1}{2},\frac{3}{2}|-1,+\frac{1}{2},-\frac{3}{2}) & (1,\frac{1}{2},\frac{3}{2}|-1,-\frac{1}{2},-\frac{3}{2}) \end{pmatrix}, \\
T^\dagger_{0} &= \begin{pmatrix} (1,\frac{1}{2},\frac{3}{2}|0,+\frac{1}{2},+\frac{3}{2}) & (1,\frac{1}{2},\frac{3}{2}|0,\frac{-1}{2},+\frac{3}{2}) \\ (1,\frac{1}{2},\frac{3}{2}|0,+\frac{1}{2},+\frac{1}{2}) & (1,\frac{1}{2},\frac{3}{2}|0,\frac{-1}{2},+\frac{1}{2}) \\ (1,\frac{1}{2},\frac{3}{2}|0,+\frac{1}{2},\frac{-1}{2}) & (1,\frac{1}{2},\frac{3}{2}|0,\frac{-1}{2},\frac{-1}{2}) \\ (1,\frac{1}{2},\frac{3}{2}|0,+\frac{1}{2},\frac{-3}{2}) & (1,\frac{1}{2},\frac{3}{2}|0,\frac{-1}{2},\frac{-3}{2}) \end{pmatrix}, \\
T^\dagger_{+1} &= \begin{pmatrix} (1,\frac{1}{2},\frac{3}{2}|+1,+\frac{1}{2},+\frac{3}{2}) & (1,\frac{1}{2},\frac{3}{2}|+1,-\frac{1}{2},+\frac{3}{2}) \\ (1,\frac{1}{2},\frac{3}{2}|+1,+\frac{1}{2},+\frac{1}{2}) & (1,\frac{1}{2},\frac{3}{2}|+1,-\frac{1}{2},+\frac{1}{2}) \\ (1,\frac{1}{2},\frac{3}{2}|+1,+\frac{1}{2},-\frac{1}{2}) & (1,\frac{1}{2},\frac{3}{2}|+1,-\frac{1}{2},-\frac{1}{2}) \\ (1,\frac{1}{2},\frac{3}{2}|+1,+\frac{1}{2},-\frac{3}{2}) & (1,\frac{1}{2},\frac{3}{2}|+1,-\frac{1}{2},-\frac{3}{2}) \end{pmatrix}.
\end{aligned} \tag{11.49}$$

The relations between the spherical basis and the isospin space for $T^\dagger$ are defined as:

$$T^\dagger_{\pm 1} = \mp \frac{T^\dagger_1 \pm T^\dagger_2}{\sqrt{2}}, \qquad T^\dagger_0 = T^\dagger_3. \tag{11.50}$$

https://doi.org/10.1017/9781108489065.012 Published online by Cambridge University Press

For the transition $I = 1/2$ to $I = 3/2$, the electromagnetic current J_μ^{EM} given in Eq. (11.13) is purely isovector in nature; hence, it may be rewritten as

$$J_\mu^{EM} = \mathcal{V}_\mu^3 = -\sqrt{\frac{3}{2}} V_\mu T_0^\dagger, \tag{11.51}$$

where we have used Eq. (11.46). The transition matrix element for the electromagnetic process $\gamma N \to R_{1/2}^{I=3/2}$, where $R_{1/2}^{I=3/2}$ represents the spin $1/2$ and isospin $3/2$ resonances, is obtained as

$$\begin{aligned}
\langle R_{1/2}^{I=3/2} |\, J_\mu^{EM} \,| N \rangle &= -\sqrt{\frac{3}{2}} \langle R_{1/2}^{I=3/2} |\, V_\mu T_0^\dagger \,| N \rangle \\
&= -\sqrt{\frac{3}{2}} \begin{pmatrix} \bar{R}_{1/2}^{++} & \bar{R}_{1/2}^{+} & \bar{R}_{1/2}^{0} & \bar{R}_{1/2}^{-} \end{pmatrix} V_\mu \begin{pmatrix} 0 & 0 \\ \sqrt{\frac{2}{3}} & 0 \\ 0 & \sqrt{\frac{2}{3}} \\ 0 & 0 \end{pmatrix} \begin{pmatrix} p \\ n \end{pmatrix} \\
&= -(\bar{R}_{1/2}^{+} V_\mu p + \bar{R}_{1/2}^{0} V_\mu n),
\end{aligned} \tag{11.52}$$

where $|R_{1/2}^{I=3/2}\rangle = \begin{pmatrix} R_{1/2}^{++} \\ R_{1/2}^{+} \\ R_{1/2}^{0} \\ R_{1/2}^{-} \end{pmatrix}$ represents the spin $1/2$ and isospin $3/2$ resonance field. From this expression, it may be noticed that the electromagnetic matrix elements and hence, the electromagnetic form factors for the proton and neutron induced isospin $3/2$ resonance excitations are the same, that is,

$$F_i^{R_{1/2}^{+}}(Q^2) = F_i^{R_{1/2}^{0}}(Q^2). \tag{11.53}$$

Using Eq. (11.46) in Eq. (11.23), the vector current for the weak charged current process is obtained as

$$V_\mu^{CC} = -\sqrt{\frac{3}{2}} (V_\mu T_1^\dagger + i V_\mu T_2^\dagger) = \sqrt{3} V_\mu T_{+1}^\dagger. \tag{11.54}$$

The transition matrix element for the weak charged current induced isospin $3/2$ resonance production on the nucleon target is written as

$$\begin{aligned}
\langle R_{1/2}^{I=3/2} |\, V_\mu^{CC} \,| N \rangle &= \langle R_{1/2}^{I=3/2} |\, \sqrt{3} V_\mu T_{+1}^\dagger \,| N \rangle, \\
&= \sqrt{3} \begin{pmatrix} \bar{R}_{1/2}^{++} & \bar{R}_{1/2}^{+} & \bar{R}_{1/2}^{0} & \bar{R}_{1/2}^{-} \end{pmatrix} V_\mu \begin{pmatrix} 1 & 0 \\ 0 & \frac{1}{\sqrt{3}} \\ 0 & 0 \\ 0 & 0 \end{pmatrix} \begin{pmatrix} p \\ n \end{pmatrix} \\
&= (\sqrt{3} \bar{R}_{1/2}^{++} V_\mu p + \bar{R}_{1/2}^{+} V_\mu n).
\end{aligned} \tag{11.55}$$

https://doi.org/10.1017/9781108489065.012 Published online by Cambridge University Press

From Eqs. (11.52) and (11.55), it may be concluded that the electromagnetic and weak currents are expressed in terms of V_μ. Therefore, for the isospin $3/2$ and spin $1/2$ resonances, the weak vector form factors for the transition $\langle R^{+}_{1/2}|\, V^{CC}_\mu\, |n\rangle$ are related to the electromagnetic form factors by the following relation:

$$F_i^{CC}(Q^2) = -F_i^{R_{1/2}}(Q^2), \tag{11.56}$$

while for the transition $\langle R^{++}_{1/2}|\, V^{CC}_\mu\, |p\rangle$, the vector form factors defined in this expression should be multiplied by $\sqrt{3}$ as shown in the first term of Eq. (11.55).

(ii) Axial vector form factors

Next, we discuss the determination of the axial vector form factors for the transition $N - R_{31}$ by the assumption of PCAC and the pion pole dominance. We proceed in a similar manner as we have done in the last section for the transition $N - R_{1/2}$. The only change is in the definition of the Lagrangian, which now becomes

$$\mathcal{L}_{NR_{1/2}\pi} = C_{\text{iso}}\, \frac{f_{NR_{1/2}\pi}}{m_\pi} \bar{\psi}_R \Gamma^\mu \partial_\mu \phi \cdot T^\dagger \psi, \tag{11.57}$$

where $C_{\text{iso}} = -\frac{1}{\sqrt{3}}$ is the isospin factor for $I = 3/2$ resonances and $T^\dagger$ is the isospin $1/2$ to $3/2$ transition operator. Using the value of C_{iso} in Eq. (11.42), the value of $F_A^{CC}(0)$ for the isospin $I = 3/2$ resonances is obtained as

$$F_A(0)|_{I=3/2} = \sqrt{\frac{2}{3}} f_\pi \frac{f_{NR_{1/2}\pi}}{m_\pi}. \tag{11.58}$$

The Q^2 dependence of the axial vector form factor $F_A^{CC}(Q^2)$ is given in Eq. (11.44) and the pseudoscalar form factor $F_P^{CC}(Q^2)$ is determined in terms of $F_A^{CC}(Q^2)$ as given in Eq. (11.45).

(iii) Determination of the strong coupling constants $f_{NR_{1/2}\pi}$

The couplings of the $NR_{1/2}\pi$ vertex for the different resonances is determined by the partial decay width of the resonance in $N\pi$. In order to determine the partial decay width of the resonance, we start with the Lagrangian given in Eq. (11.34). From the expression of the Lagrangian, it may be observed that different isospins ($I = 1/2, 3/2$) of resonance yield different expressions of decay width but the spin of the resonance does not play any role in the Lagrangian or in the decay width. In the following, we present in detail the evaluation of the decay width of the spin $1/2$ resonances with isospin $1/2$.

The scalar product of the derivative pion field with the Pauli matrices yields

$$\partial_\mu \vec{\phi} \cdot \vec{\tau} = \partial_\mu \phi_1 \tau_1 + \partial_\mu \phi_2 \tau_2 + \partial_\mu \phi_3 \tau_3 = \sqrt{2}(\partial_\mu \phi_+ \tau_- + \partial_\mu \phi_- \tau_+) + \partial_\mu \phi_0 \tau_0, \tag{11.59}$$

where the last expression in Eq. (11.59) represents the scalar product in spherical basis. $\tau_\pm$ and $\phi_\pm$ are defined as

$$\tau_\pm = \frac{1}{2}(\tau_1 \pm i\tau_2), \qquad \tau_0 = \tau_3, \tag{11.60}$$

https://doi.org/10.1017/9781108489065.012 Published online by Cambridge University Press

$$\phi_\pm = \frac{1}{\sqrt{2}}(\phi_1 \pm i\phi_2), \qquad \phi_0 = \phi_3. \tag{11.61}$$

The complex pion field $\phi(x)$ represents particles with charge $|e|$ and antiparticles with charge $-|e|$. The field operator $\hat{\phi}(x)$ is given as:

$$\hat{\phi}(x) = \int \frac{d^3k}{(2\pi)^{3/2}\sqrt{2\omega_k}}\left[\hat{a}(\vec{k})e^{-ik\cdot x} + \hat{b}^\dagger(\vec{k})e^{ik\cdot x}\right], \tag{11.62}$$

and the adjoint of the field operator $\hat{\phi}^\dagger(x)$ is given as

$$\hat{\phi}^\dagger(x) = \int \frac{d^3k}{(2\pi)^{3/2}\sqrt{2\omega_k}}\left[\hat{a}^\dagger(\vec{k})e^{ik\cdot x} + \hat{b}(\vec{k})e^{-ik\cdot x}\right]. \tag{11.63}$$

The operator $\hat{a}(\vec{k})$ annihilates a particle with momentum $\vec{k}$; $\hat{b}^\dagger(\vec{k})$ creates a particle; $\hat{a}^\dagger(\vec{k})$ annihilates an antiparticle; and $\hat{b}(\vec{k})$ creates an antiparticle. ϕ_- given in Eq. (11.61) creates a π^- or annihilates a π^+; ϕ_+ creates a π^+ or annihilates a ϕ_-; and ϕ_0 creates or annihilates a π^0, which has been discussed in detail in Chapter 2.

Using Eq. (11.59) in Eq. (11.34), the Lagrangian for the $NR_{1/2}\pi$ vertex becomes

$$\begin{aligned}
\mathcal{L}_{NR_{1/2}\pi} &= \frac{f_{NR_{1/2}\pi}}{m_\pi}\bar{\psi}_R\Gamma^\mu(\sqrt{2}(\partial_\mu\phi_+\tau_- + \partial_\mu\phi_-\tau_+) + \partial_\mu\phi_3\tau_3)\psi, \\
&= \frac{f_{NR_{1/2}\pi}}{m_\pi}\langle R_{1/2}|\,\Gamma^\mu\begin{pmatrix}\partial_\mu\phi_0 & \sqrt{2}\partial_\mu\phi_- \\ \sqrt{2}\partial_\mu\phi_+ & -\partial_\mu\phi_0\end{pmatrix}|N\rangle, \\
&= \frac{f_{NR_{1/2}\pi}}{m_\pi}[\bar{R}^+_{1/2}\Gamma^\mu\partial_\mu\phi_0 p + \sqrt{2}\bar{R}^+_{1/2}\Gamma^\mu\partial_\mu\phi_+ n + \bar{R}^0_{1/2}\Gamma^\mu\partial_\mu\phi_- p \\
&\quad -\bar{R}^0_{1/2}\Gamma^\mu\partial_\mu\phi_0 n].
\end{aligned} \tag{11.64}$$

In Eq. (11.64), the first term on the right-hand side represents the absorption of a π^0 by the proton to produce a spin $1/2$ resonance with positive charge. Similarly, one may identity the different transitions represented by the different terms in Eq. (11.64). Now, focusing on the first term of the Lagrangian given in Eq. (11.64), that is,

$$\mathcal{L}_{NR_{1/2}\pi} = \frac{f_{NR_{1/2}\pi}}{m_\pi}\bar{R}^+_{1/2}\Gamma^\mu\partial_\mu\phi_0 p, \tag{11.65}$$

we can evaluate the decay width of the resonance. The Hermitian conjugate of the Lagrangian can be written as

$$L^{h.c.}_{NR_{\frac{1}{2}}\pi} = \frac{f_{NR_{1/2}\pi}}{m_\pi}\bar{p}\Gamma^\mu\partial_\mu\phi_0^\dagger R^+_{1/2}. \tag{11.66}$$

$\Gamma^\mu = \gamma^\mu\gamma_5$ (γ^μ) for the positive (negative) parity resonances. In the following, we present the evaluation of the decay width considering the negative parity resonances. However, one may

https://doi.org/10.1017/9781108489065.012 Published online by Cambridge University Press

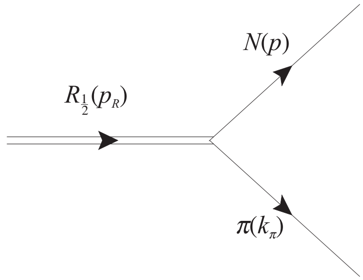

Figure 11.8 Feynman diagram for the decay of a spin $1/2$ resonance to a nucleon and a pion. The quantities in the parentheses represent the four momenta of the corresponding particles.

obtain similar results while considering positive parity resonances and the expression for the decay width is given in terms of both positive and negative parity resonances.

Using Eqs. (11.65) and (11.66) and applying Feynman rules, the transition matrix element for the process $R_{1/2}(p_R) \to N(p) + \pi(k_\pi)$ as shown in Figure 11.8, is written as

$$\mathcal{M} = \frac{i f_{NR_{1/2}\pi}}{m_\pi} \bar{u}(p)\gamma_\mu k_\pi^\mu u(p_R). \tag{11.67}$$

The spin averaged transition matrix element squared is obtained as

$$\begin{aligned}\overline{\sum}\sum|\mathcal{M}|^2 &= \frac{1}{2}\left(\frac{f_{NR_{1/2}\pi}}{m_\pi}\right)^2 k_\pi^\mu k_\pi^\nu |\bar{u}(p)\gamma_\mu u(p_R)|^2 \\ &= \frac{1}{2}\left(\frac{f_{NR_{1/2}\pi}}{m_\pi}\right)^2 k_\pi^\mu k_\pi^\nu [\mathrm{Tr}(\gamma_\mu(\not{p}_R + M_R)\gamma_\nu(\not{p} + M))] \\ &= 2\left(\frac{f_{NR_{1/2}\pi}}{m_\pi}\right)^2 (2p_R \cdot k_\pi p \cdot k_\pi - m_\pi^2(p_R \cdot p - MM_R)).\end{aligned} \tag{11.68}$$

Using the expression of the two-body decay Γ given in Appendix E, we get

$$\frac{d\Gamma}{d\Omega_\pi} = \frac{|\vec{k}_\pi|}{32\pi^2 M_R^2} \overline{\sum}\sum|\mathcal{M}|^2. \tag{11.69}$$

In this expression of Γ, we have to perform the integration over the solid angle of the pion, but the transition matrix element squared given in Eq. (11.68), when evaluated in the resonance rest frame ($\vec{p}_R = 0$), does not contain any angular dependence. Thus, the following formula for the width is obtained:

$$\Gamma = \frac{|\vec{k}_\pi^{\mathrm{CM}}|}{8\pi M_R^2}\left(2\left(\frac{f_{NR_{1/2}\pi}}{m_\pi}\right)^2 (2p_R \cdot k_\pi p \cdot k_\pi - m_\pi^2(p_R \cdot p - MM_R))\right), \tag{11.70}$$

$|\vec{k}_\pi^{\mathrm{CM}}|$ represents the momentum of the outgoing pion in the resonance rest frame. Substituting $k_\pi = p_R - p$ in these expressions yields the decay width in terms of p_R and p. The scalar

https://doi.org/10.1017/9781108489065.012 Published online by Cambridge University Press

product of p_R with p gives $p_R \cdot p = E_N M_R$, where E_N is the energy of the outgoing nucleon in the resonance rest frame. With these simplifications, Eq. (11.70) can be rewritten as

$$\begin{aligned}\Gamma_{R_{1/2}\to N\pi} &= \frac{1}{4\pi M_R^2}\left(\frac{f_{NR_{1/2}\pi}}{m_\pi}\right)^2 |\vec{k}_\pi^{\rm CM}| \left[2(p_R^2 - p_R\cdot p)(p_R\cdot p - p^2) - m_\pi^2 M_R E_N + m_\pi^2 M M_R\right] \\ &= \frac{I_R}{4\pi M_R}\left(\frac{f_{NR_{1/2}\pi}}{m_\pi}\right)^2 |\vec{k}_\pi^{\rm CM}|(M_R - M)^2(E_N + M), \qquad (11.71)\end{aligned}$$

where I_R is the isospin factor and is equal to 1 (3) for the isospin $3/2$ $(1/2)$ resonances.

Now, for positive parity resonances, the expression for the decay width is given as

$$\Gamma_{R_{1/2}\to N\pi} = \frac{I_R}{4\pi M_R}\left(\frac{f_{NR_{1/2}\pi}}{m_\pi}\right)^2 |\vec{k}_\pi^{\rm CM}|(M_R + M)^2(E_N - M), \qquad (11.72)$$

where

$$E_N = \frac{W^2 + M^2 - m_\pi^2}{2M_R}, \qquad (11.73)$$

$$|\vec{k}_\pi^{\rm CM}| = \frac{\sqrt{(W^2 - m_\pi^2 - M^2)^2 - 4m_\pi^2 M^2}}{2M_R}. \qquad (11.74)$$

W is the total center of mass energy carried by the resonance.

11.2.2 CC excitation of spin $3/2$ resonances

Excitation of spin $3/2$ and isospin $1/2$ R_{13} resonances

The basic reactions for the (anti)neutrino induced spin $3/2$ resonance excitations on the nucleon target, shown in the left-hand side of Figure 11.9, are written as:

$$\nu_l(\bar{\nu}_l)\ (k) + N(p) \longrightarrow l^-(l^+)\ (k') + R_{3/2}(p_R) \qquad (11.75)$$

for which the transition amplitude is written as

$$\mathcal{M} = \frac{G_F}{\sqrt{2}} \cos\theta_C\ l_\mu\ J^{\mu CC}_{\frac{3}{2}}, \qquad (11.76)$$

where the leptonic current is the same as given in Eq. (11.3) and the general structure for the hadronic current for spin 3/2 resonance excitation is written as [294]:

$$J^{\mu CC}_{\frac{3}{2}} = \bar{\psi}_\nu(p')\Gamma^{\nu\mu}_{\frac{3}{2}} u(p). \qquad (11.77)$$

Here $\psi^\mu(p)$ is the Rarita–Schwinger spinor for the spin 3/2 resonances and $\Gamma^{\frac{3}{2}}_{\nu\mu}$ has the following general structure for the positive and negative parity resonance states:

$$\Gamma^{\frac{3}{2}^+}_{\nu\mu} = \left[V^{\frac{3}{2}}_{\nu\mu} - A^{\frac{3}{2}}_{\nu\mu}\right]\gamma_5, \qquad (11.78)$$

$$\Gamma^{\frac{3}{2}^-}_{\nu\mu} = V^{\frac{3}{2}}_{\nu\mu} - A^{\frac{3}{2}}_{\nu\mu}, \qquad (11.79)$$

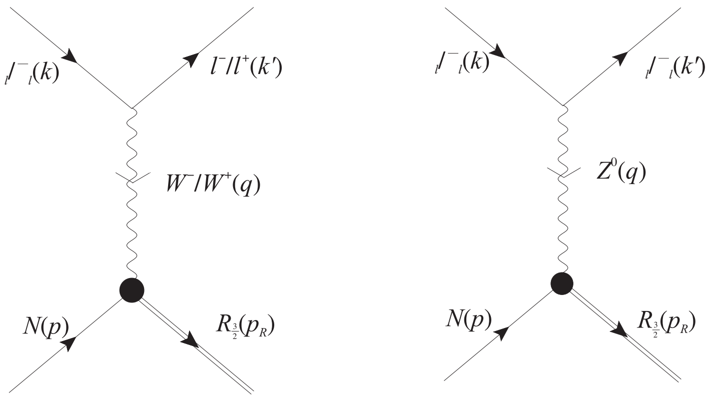

Figure 11.9 Feynman diagram for the charged current (left) and neutral current (right) induced spin 3/2 resonance production. The quantities in the parentheses represent the four momenta of the corresponding particles.

where $V_{\frac{3}{2}}$ $(A_{\frac{3}{2}})$ is the vector (axial vector) current for spin 3/2 resonances and are given by

$$V^{\frac{3}{2}}_{\nu\mu} = \left[\frac{C_3^V}{M}(g_{\mu\nu} - q_\nu\gamma_\mu) + \frac{C_4^V}{M^2}(g_{\mu\nu}q\cdot p' - q_\nu p'_\mu) + \frac{C_5^V}{M^2}(g_{\mu\nu}q\cdot p - q_\nu p_\mu) + g_{\mu\nu}C_6^V\right], \tag{11.80}$$

$$A^{\frac{3}{2}}_{\nu\mu} = -\left[\frac{C_3^A}{M}(g_{\mu\nu} - q_\nu\gamma_\mu) + \frac{C_4^A}{M^2}(g_{\mu\nu}q\cdot p' - q_\nu p'_\mu) + C_5^A g_{\mu\nu} + \frac{C_6^A}{M^2}q_\nu q_\mu\right]\gamma_5. \tag{11.81}$$

In this expression, C_i^V and C_i^A are the vector and axial vector charged current transition form factors which are functions of Q^2.

(i) Vector form factors

The vector current for the R_{13} resonances is given in Eq. (11.80) with corresponding form factors C_i^V defined for each resonances. The hypothesis of CVC leads to $C_6^V(Q^2) = 0$. The determination of the weak vector form factors in terms of the electromagnetic form factors depends upon the isospin structure of the current. For isospin $1/2$ resonances, the relation between the weak vector form factor and the electromagnetic form factors is given by Eq. (11.9). Similarly, for the isospin $3/2$ resonances, the relation is given by Eq. (11.56). The isovector $C_i^V(Q^2), i = 3,4,5$ form factors for any $J = \frac{3}{2}$, $I = \frac{1}{2}$ resonance like $D_{13}(1520)$, $P_{13}(1720)$, etc., are written as [482],

$$C_i^V(Q^2) = C_i^{R^+}(Q^2) - C_i^{R^0}(Q^2), \qquad i = 3,4,5. \tag{11.82}$$

https://doi.org/10.1017/9781108489065.012 Published online by Cambridge University Press

The electromagnetic vector form factors $C_i^{R^+,R^0}(Q^2)$, $(i = 3,4,5)$ are derived from the helicity amplitudes $A_{1/2}$, $A_{3/2}$, and $S_{1/2}$ following the same formalism as discussed earlier for the spin 1/2 resonances in Section 11.2.1.

In the case of spin 3/2 resonances, along with $J_z^R = +1/2$ (as shown in Figure 11.4), $J_z^R = +3/2$ also contribute in the positive Z-direction as depicted in Figure 11.10. Again it is our choice to fix J_z^R in the positive Z-direction; one may obtain the expressions for the helicity amplitudes by fixing J_z^R in the negative Z-direction. The expressions for $A_{1/2}$ and $S_{1/2}$ are given in Eqs. (11.25) and (11.26) with $\Gamma_\mu \simeq V_\mu$ defined in Eqs. (11.78), (11.79) and (11.80), respectively, for the positive and negative parity resonance. The expression for $A_{3/2}$ is given as:

$$A_{3/2}^N = \sqrt{\frac{2\pi\alpha}{K_R}} \langle R, J_z^R = +3/2 | \epsilon_\mu^+ \Gamma^\mu | N, J_z^N = +1/2 \rangle \zeta, \tag{11.83}$$

where the variables in Eq. (11.83) are already defined in Section 11.2.1.

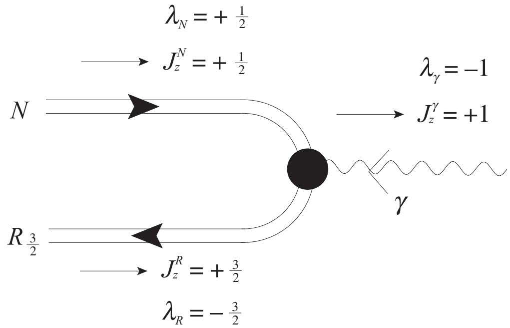

Figure 11.10 Diagrammatic representation of the helicity amplitude, $A_{3/2}$ for spin 3/2 resonances.

The explicit relations between the form factors $C_i^{R^+,R^0}(Q^2)$ and the helicity amplitudes $A_{1/2,3/2}^{p,n}(Q^2)$ and $S_{\frac{1}{2}}^{p,n}(Q^2)$ are given by [483]

$$A_{\frac{3}{2}}^{p,n}(Q^2) = \sqrt{\frac{\pi\alpha}{M}\frac{(M_R \mp M)^2 + Q^2}{M_R^2 - M^2}} \left[\frac{C_3^{R^+,R^0}(Q^2)}{M}(M \pm M_R) \right.$$
$$\left. \pm \frac{C_4^{R^+,R^0}(Q^2)}{M^2}\frac{M_R^2 - M^2 - Q^2}{2} \pm \frac{C_5^{R^+,R^0}(Q^2)}{M^2}\frac{M_R^2 - M^2 + Q^2}{2} \right], \tag{11.84}$$

$$A_{\frac{1}{2}}^{p,n}(Q^2) = \sqrt{\frac{\pi\alpha}{3M}\frac{(M_R \mp M)^2 + Q^2}{M_R^2 - M^2}} \left[\frac{C_3^{R^+,R^0}(Q^2)}{M}\frac{M^2 + MM_R + Q^2}{M_R} - \frac{C_4^{R^+,R^0}(Q^2)}{M^2} \right.$$
$$\left. \times \frac{M_R^2 - M^2 - Q^2}{2} - \frac{C_5^{R^+,R^0}(Q^2)}{M^2}\frac{M_R^2 - M^2 + Q^2}{2} \right], \tag{11.85}$$

$$S_{\frac{1}{2}}^{p,n}(Q^2) = \pm\sqrt{\frac{\pi\alpha}{6M}\frac{(M_R \mp M)^2 + Q^2}{M_R^2 - M^2}} \frac{\sqrt{Q^4 + 2Q^2(M_R^2 + M^2) + (M_R^2 - M^2)^2}}{M_R^2}$$
$$\times \left[\frac{C_3^{R^+,R^0}(Q^2)}{M}M_R + \frac{C_4^{R^+,R^0}(Q^2)}{M^2}M_R^2 + \frac{C_5^{R^+,R^0}(Q^2)}{M^2}\frac{M_R^2 + M^2 + Q^2}{2} \right], \tag{11.86}$$

https://doi.org/10.1017/9781108489065.012 Published online by Cambridge University Press

where the upper (lower) sign represents the positive (negative) parity resonance state, M_R is the mass of the corresponding resonance, $A_{\frac{3}{2},\frac{1}{2}}(Q^2)$ and $S_{\frac{1}{2}}(Q^2)$ are the amplitudes corresponding to the transverse and longitudinal polarizations of the photon, respectively, and are parameterized at different Q^2 using Eq. (11.31).

The Q^2 dependence of the helicity amplitudes is parameterized by MAID (Eq. (11.31)). The values of the parameters appearing in Eq. (11.31) for the spin $3/2$ resonances are presented in Tables 11.8 and 11.9 for the proton and neutron targets, respectively. As already mentioned, for the isospin $3/2$ resonances, the different parameters for $A_{1/2,3/2}$ and $S_{1/2}$ given in Eq. (11.31) have the same values for the proton and neutron targets.

Table 11.8 MAID parameterization [493] of the transition form factors for the spin $3/2$ resonance on a proton target. Different components of this table have the same meaning as in Table 11.6.

N^*	Amplitude	$\mathcal{A}_\alpha(0)$	a_1	a_2	a_4	b_1
$D_{13}(1520)$	$A_{\frac{1}{2}}$	-27.4	8.580	-0.252	0.357	1.20
	$A_{\frac{3}{2}}$	160.6	-0.820	0.541	-0.016	1.06
	$S_{\frac{1}{2}}$	-63.5	4.19	0	0	3.40
$D_{33}(1700)$	$A_{\frac{1}{2}}$	226.0	1.91	0	0	1.77
	$A_{\frac{3}{2}}$	210.0	0.88	1.71	0	2.02
	$S_{\frac{1}{2}}$	2.1	0	0	0	2.0
$P_{13}(1720)$	$A_{\frac{1}{2}}$	73.0	1.89	0	0	1.55
	$A_{\frac{3}{2}}$	-11.5	10.83	-0.66	0	0.43
	$S_{\frac{1}{2}}$	-53.0	2.46	0	0	1.55

Table 11.9 MAID [493] parameterization for neutron target ($a_{2,3,4} = 0$) for spin $3/2$ resonances.

N^*	Amplitude	$\mathcal{A}_\alpha(0)$	a_1	b_1
$D_{13}(1520)$	$A_{\frac{1}{2}}$	-76.5	-0.53	1.55
	$A_{\frac{3}{2}}$	-154.0	0.58	1.75
	$S_{\frac{1}{2}}$	13.6	15.7	1.57
$P_{13}(1720)$	$A_{\frac{1}{2}}$	-2.9	12.7	1.55
	$A_{\frac{3}{2}}$	-31.0	5.00	1.55
	$S_{\frac{1}{2}}$	0	0	0

(ii) Axial vector form factors

The form factors $C_i^A(Q^2)$, $(i = 3,4,5,6)$ corresponding to the axial vector current have not been studied in the case of higher resonances except for $P_{33}(1232)$ resonance. However, in the literature, PCAC and the Goldberger–Treiman relation are used to determine $C_5^A(Q^2)$ and $C_6^A(Q^2)$; the other form factors are taken to be zero. The divergence of the axial vector current given in Eq. (11.81) yields

$$
\begin{aligned}
\partial_\mu A^\mu_{3/2\pm} &= -iq_\mu A^\mu_{3/2\pm} \\
&= -i\bar{u}_\nu(p_R)\left[C_5^A q^\nu + \frac{C_6^A}{M^2}q^2 q^\nu\right]\Gamma u(p), \\
&= -i\bar{u}_\nu(p_R)q^\nu\left[C_5^A + \frac{C_6^A}{M^2}q^2\right]\Gamma u(p),
\end{aligned} \tag{11.87}
$$

where $\Gamma = 1$ (γ_5) for positive (negative) parity resonances. Now, we evaluate the pion pole contribution of the axial vector current and relate it with the second term in Eq. (11.87), which is identified as the induced pseudoscalar form factor.

We have discussed in detail the contribution of the pion pole in the case of the spin $1/2$ resonances in Section 11.2.1. Following the same analogy, the matrix element for the process $N \to R_{3/2}l\nu$ (depicted in Figure 11.5) in the pion pole dominance is written as

$$
A_\mu = (A^{N\to R_{3/2}\pi}) \times \left(\frac{i}{k_\pi^2 - m_\pi^2}\right) \times (-i\sqrt{2}f_\pi k_\pi^\mu). \tag{11.88}
$$

The current $A^{N\to R_{3/2}\pi}$ at the $NR_{3/2}\pi$ vertex is determined by the following Lagrangian

$$
\mathcal{L}_{NR_{3/2}\pi} = C_{\text{iso}}\,\frac{f_{NR_{3/2}\pi}}{m_\pi}\bar{\psi}^\mu_R\,\Gamma\,\partial_\mu\vec{\phi}\cdot\vec{\tau}\,\psi \tag{11.89}
$$

where $C_{\text{iso}} = \sqrt{2}$ is the isospin factor. $f_{NR_{3/2}\pi}$ is the coupling of the $NR_{3/2}\pi$ vertex which is obtained using the partial decay width of $R_{3/2} \to N\pi$ and is later discussed in the text. $\Gamma = 1(\gamma_5)$ stands for the positive (negative) parity resonances and τ represents the Pauli spin matrices. Using the Lagrangian given in Eq. (11.89), the axial vector current for the $N(p) \to R_{3/2}(p_R) + \pi(k_\pi)$ vertex is written as

$$
A^{N\to R_{3/2}\pi} = -i\bar{u}_\mu(p_R)\left(C_{\text{iso}}\frac{f_{NR_{3/2}\pi}}{m_\pi}\Gamma\partial^\mu\phi\right)u(p). \tag{11.90}
$$

Using Eq. (11.90) in Eq. (11.88), the transition matrix element for the process $N \to R_{3/2}l\nu$ in the pion pole dominance is obtained as

$$
\begin{aligned}
A^\mu &= -iC_{\text{iso}}\,\bar{u}_\alpha(p_R)\frac{f_{NR_{3/2}\pi}}{m_\pi}\Gamma\partial^\alpha\phi u(p)\,\frac{\sqrt{2}f_\pi k_\pi^\mu}{k_\pi^2 - m_\pi^2} \\
&= -C_{\text{iso}}\frac{f_{NR_{3/2}\pi}}{m_\pi}\,\bar{u}_\alpha(p_R)\Gamma k_\pi^\alpha u(p)\,\frac{\sqrt{2}f_\pi k_\pi^\mu}{k_\pi^2 - m_\pi^2},
\end{aligned} \tag{11.91}
$$

with $q^\mu = p_R^\mu - p^\mu = k_\pi^\mu$. Comparing Eq. (11.91) with the last term (pseudoscalar form factor C_6^A) of Eq. (11.81), we obtain

$$
C_6^A = -C_{\text{iso}}\,\sqrt{2}f_\pi\frac{f_{NR_{3/2}\pi}}{m_\pi}\frac{M^2}{Q^2 + m_\pi^2}. \tag{11.92}
$$

Using the value of C_6^A as obtained here in Eq. (11.87), we get

$$\partial_\mu A^\mu_{3/2\pm} \;=\; i\bar{u}_\nu(p_R)q^\nu \left[C_5^A - C_{\text{iso}}\,\sqrt{2}f_\pi \frac{f_{NR_{3/2}\pi}}{m_\pi}\frac{1}{Q^2+m_\pi^2}q^2\right]\Gamma u(p). \tag{11.93}$$

In the chiral limit ($Q^2 + m_\pi^2 \sim Q^2$), this expression reduces to

$$\partial_\mu A^\mu_{3/2\pm} \;=\; i\bar{u}_\nu(p_R)q^\nu \left[C_5^A + C_{\text{iso}}\,\sqrt{2}f_\pi \frac{f_{NR_{3/2}\pi}}{m_\pi}\right]\Gamma u(p). \tag{11.94}$$

The chiral limit demands that $\partial_\mu A^\mu_{1/2\pm} = 0$, and one may relate C_5^A with $f_{NR_{1/2}\pi}$ as

$$C_5^A \;=\; -C_{\text{iso}}\,\sqrt{2}f_\pi \frac{f_{NR_{3/2}\pi}}{m_\pi}, \tag{11.95}$$

which is nothing but the Goldberger–Treiman relation for the spin $3/2$ resonances.

Using the value of C_{iso} as given here, $C_5^A(0)$ for the isospin $1/2$ resonances are obtained as:

$$C_5^A(0)\Big|_{I=1/2} \;=\; -2f_\pi \frac{f_{NR_{3/2}\pi}}{m_\pi}. \tag{11.96}$$

In the case of higher resonances, the information about the Q^2 dependence of the axial vector form factor $C_5^A(Q^2)$ is scarce; therefore, a dipole parameterization, is generally assumed:

$$C_5^A(Q^2) = C_5^A(0)\left(1+\frac{Q^2}{M_{AR}^2}\right)^{-2} \tag{11.97}$$

with $M_{AR} = 1$ GeV. However, deviations from the dipole have also been discussed by many authors [484].

Using Eq. (11.95) in Eq. (11.92), the pseudoscalar form factor $C_6(Q^2)$ is obtained in terms of $C_5(Q^2)$ as

$$C_6^A(Q^2) = \frac{M^2}{Q^2+m_\pi^2}C_5^A(Q^2). \tag{11.98}$$

$C_3^A(Q^2)$ and $C_4^A(Q^2)$ are taken to be 0. The Q^2 dependence of the form factors, thus, obtained are shown in Figures 11.11 and 11.12, respectively, for $D_{13}(1520)$ and $P_{13}(1720)$ resonances.

Excitation of spin $3/2$ and isospin $3/2$ resonances

(i) Vector form factors for Δ resonance

In this section, we discuss the vector and axial vector form factors for the Δ resonance, which is the most studied resonance theoretically as well as experimentally. In the next sections, we discuss the parameterization of the vector and axial vector form factors for the other spin $3/2$ resonances. From the CVC hypothesis, one takes $C_6^V(Q^2) = 0$. The three vector form factors $C_i^V(Q^2), i = 3, 4, 5$, for the $\Delta(1232)$ resonance are given in terms of the isovector

https://doi.org/10.1017/9781108489065.012 Published online by Cambridge University Press

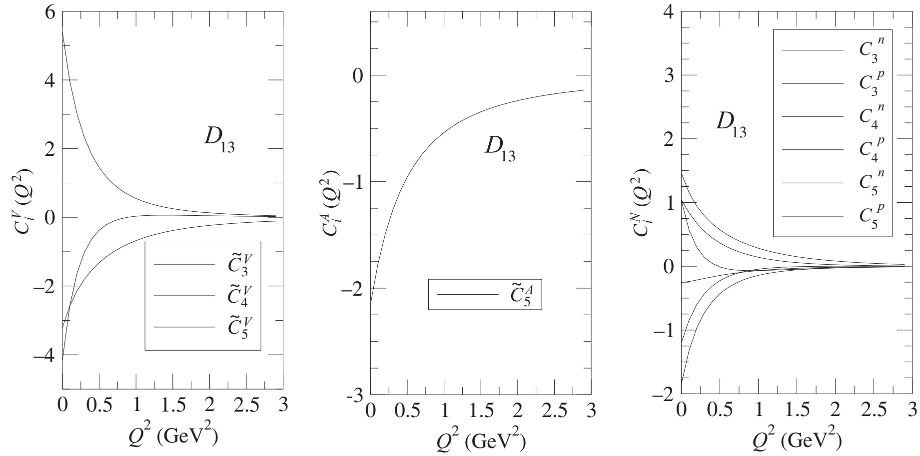

Figure 11.11 Q^2 dependence of different form factors of D_{13} resonance. From left to right panel: C_3^V, C_4^V, and C_5^V as mentioned in Eq. (11.82); C_5^A as mentioned in Eq. (11.97); and $C_i^{n,p}, i = 3,4,5$ as mentioned in Eqs. (11.84)–(11.86).

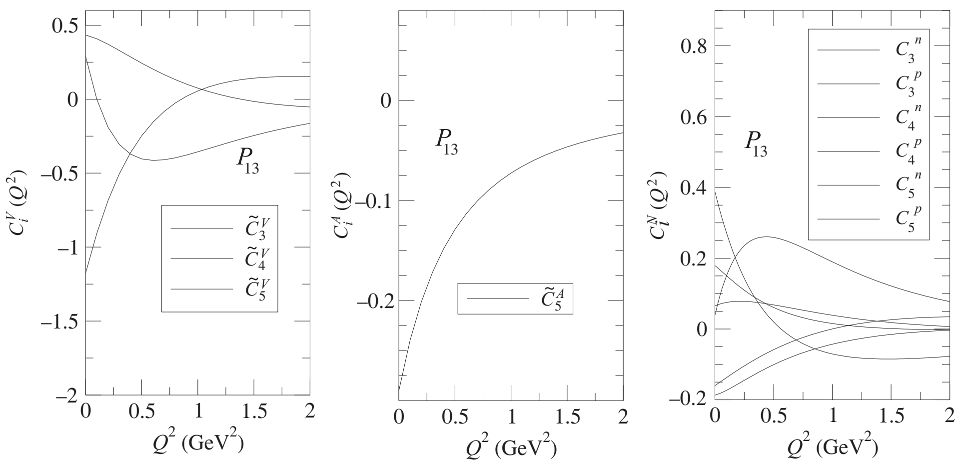

Figure 11.12 Q^2 dependence of different form factors of P_{13} resonance. From left to right panel: C_3^V, C_4^V, and C_5^V as mentioned in Eq. (11.82); C_5^A as mentioned in Eq. (11.97); and $C_i^{n,p}, i = 3,4,5$ as mentioned in Eqs. (11.84)–(11.86).

electromagnetic form factors for $p \to \Delta^+$ transition and the parameterization which are taken from the Ref. [484],

$$C_3^V(Q^2) = \frac{2.13}{\left(1+\frac{Q^2}{M_V^2}\right)^2} \times \frac{1}{1+\frac{Q^2}{4M_V^2}},$$

$$C_4^V(Q^2) = \frac{-1.51}{\left(1+\frac{Q^2}{M_V^2}\right)^2} \times \frac{1}{1+\frac{Q^2}{4M_V^2}},$$

https://doi.org/10.1017/9781108489065.012 Published online by Cambridge University Press

$$C_5^V(Q^2) \quad = \quad \frac{0.48}{\left(1+\frac{Q^2}{M_V^2}\right)^2} \times \frac{1}{1+\frac{Q^2}{0.776M_V^2}}, \tag{11.99}$$

with the vector dipole mass taken as $M_V = 0.84$ GeV. From the isospin analysis, it can be shown easily that

$$(C_i^V)_{\Delta^{++}} = \sqrt{3}(C_i^V)_{\Delta^+}. \tag{11.100}$$

(ii) Axial vector form factors for Δ resonance

The axial vector form factors $C_i^A(Q^2)$, $(i = 3, 4, 5)$ are generally determined by using the hypothesis of PCAC with pion pole dominance through the off diagonal Goldberger–Treiman relation or obtained in quark model calculations [494, 495]. The earliest model used to determine the axial vector form factors was the Adler's model [464], and was applied by Schreiner and von Hippel [471]; the model was consistent in a way with the hypothesis of PCAC and generalized Goldberger– Treiman relation. These considerations give $C_6^A(Q^2)$ in terms of $C_5^A(Q^2)$ using generalized Goldberger-Treiman relation [471]:

$$C_6^A(Q^2) = C_5^A(Q^2)\frac{M^2}{Q^2+m_\pi^2}, \tag{11.101}$$

$$C_5^A(0) = f_\pi \frac{f_{\Delta N\pi}}{2\sqrt{3}M}, \tag{11.102}$$

where $f_{\Delta N\pi}$ is the $\Delta N\pi$ coupling strength for $\Delta \to N\pi$ decay.

The Q^2 dependence of $C_3^A(Q^2)$ and $C_4^A(Q^2)$ obtained in Adler's model are given as [464, 471]:

$$C_4^A(Q^2) = -\frac{1}{4}C_5^A(Q^2); \qquad C_3^A(Q^2) = 0. \tag{11.103}$$

The Q^2 dependence of C_5^A has been parameterized by Schreiner and von Hippel [471] in Adler's model [464] and is given by

$$C_5^A(Q^2) \quad = \quad \frac{C_5^A(0)\left(1+\frac{a\,Q^2}{b+Q^2}\right)}{\left(1+Q^2/M_{A\Delta}^2\right)^2}, \tag{11.104}$$

where a and b are unknown parameters which are determined from experiments and found to be $a = -1.21$ and $b = 2$ GeV^2 [458, 459]. $M_{A\Delta}$ is the axial dipole mass.

Most of the recent theoretical calculations [481, 482, 484, 485] use a simpler modification to the dipole form, viz.,

$$C_5^A(Q^2) = \frac{C_5^A(0)}{\left(1+Q^2/M_{A\Delta}^2\right)^2}\,\frac{1}{1+Q^2/(3M_{A\Delta}^2)}. \tag{11.105}$$

https://doi.org/10.1017/9781108489065.012 Published online by Cambridge University Press

$M_{A\Delta}$ is generally chosen to be 1.026 GeV corresponding to the world average value obtained from the experimental analysis of quasielastic scattering events [443].

(iii) Vector form factors

The vector current for the spin $3/2$ and isospin $3/2$ resonances is given in Eq. (11.80) with corresponding form factors C_i^V defined for each resonances. The hypothesis of CVC leads to $C_6^V(Q^2) = 0$. The weak vector form factors $C_i^V(Q^2)$ are related to the electromagnetic ones by the following relations

$$C_i^V(Q^2) = -C_i^R(Q^2), \qquad i = 3,4,5, \tag{11.106}$$

for $R^+_{3/2}$ production. For the $R^{++}_{3/2}$ production, the form factors given in Eq. (11.106) should be multiplied by $\sqrt{3}$.

(iv) Axial vector form factors

Next, we discuss the determination of the axial vector form factors for the transition of $N - R_{33}$. We proceed in a similar manner as done in the last section for spin $3/2$ and isospin $1/2$ resonances; the only change is in the definition of the Lagrangian, which now becomes

$$\mathcal{L}_{NR_{3/2}\pi} = C_{\text{iso}} \frac{f_{NR_{3/2}\pi}}{m_\pi} \bar{\psi}_R^\mu \Gamma \partial_\mu \vec{\phi} \cdot \vec{T}^\dagger \psi \tag{11.107}$$

where $C_{\text{iso}} = -\frac{1}{\sqrt{3}}$ is the isospin factor for the $I = 3/2$ resonances; $T^\dagger$ is the isospin $1/2$ to $3/2$ transition operator. Using the value of C_{iso} in Eq. (11.42), the value of $C_5^A(0)$ for R_{33} resonances is obtained as

$$C_5^A(0)\Big|_{I=3/2} = \sqrt{\frac{2}{3}} f_\pi \frac{f_{NR_{3/2}\pi}}{m_\pi}. \tag{11.108}$$

The Q^2 dependence of the axial vector form factor $C_5^A(Q^2)$ is given in Eq. (11.97) and the pseudoscalar form factor $C_6^A(Q^2)$ is determined in terms of $C_5^A(Q^2)$ as given in Eq. (11.98).

(v) Determination of the coupling constants

The couplings $f_{NR_{3/2}\pi}$ of the $NR_{3/2}\pi$ vertex are determined in terms of the partial decay width of the resonance in $N\pi$. We follow the same procedure as we have done for the determination of $f_{NR_{1/2}\pi}$ in Section 11.2.1. The Lagrangian for the $NR_{3/2}\pi$ vertex given in Eq. (11.89) contains the isospin factor $t = \tau$ $(T^\dagger)$ for $I = 1/2$ $(3/2)$ resonances but no explicit dependence of spin on the Lagrangian is observed. In the following, we discuss in detail the evaluation of the decay width of the spin $3/2$ resonances with isospin $3/2$, where $t = T^\dagger$.

The scalar product of the derivative pion field with the isospin $1/2 \to 3/2$ transition operator $T^\dagger$, yields

$$\begin{aligned} \partial_\mu \vec{\phi} \cdot \vec{T}^\dagger &= \partial_\mu \phi_1 T_1^\dagger + \partial_\mu \phi_2 T_2^\dagger + \partial_\mu \phi_3 T_3^\dagger, \\ &= \partial_\mu \phi_+ T_{-1}^\dagger - \partial_\mu \phi_- T_{+1}^\dagger + \partial_\mu \phi_0 T_0^\dagger, \end{aligned} \tag{11.109}$$

https://doi.org/10.1017/9781108489065.012 Published online by Cambridge University Press

where the last expression in the equation represents the scalar product in spherical basis. $\phi_{\pm,0}$ and $T^{\dagger}_{\pm,0}$ are defined in Eqs. (11.61) and (11.50), respectively.

Using Eq. (11.109) in Eq. (11.89), the Lagrangian for the $NR_{3/2}\pi$ vertex becomes (Figure 11.13)

$$\mathcal{L}_{NR_{3/2}\pi} = C_{\text{iso}} \frac{f_{NR_{3/2}\pi}}{m_\pi} \langle R^{\mu}_{3/2}| \Gamma(\partial_\mu\phi_+ T^{\dagger}_{-1} - \partial_\mu\phi_- T^{\dagger}_{+1} + \partial_\mu\phi_0 T^{\dagger}_0) |N\rangle \, , \quad (11.110)$$

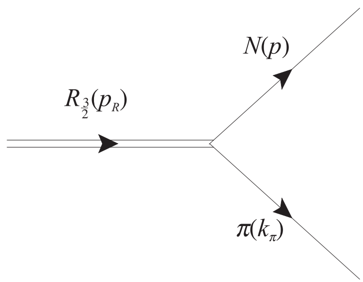

Figure 11.13 Feynman diagram for the decay of a spin 3/2 resonance in a nucleon and a pion. The quantities in the parentheses represent the four momenta of the corresponding particles.

where the matrices $T^{\dagger}_{\pm1,0}$ are defined in Eq. (11.49). Let us focus on the second term of the Lagrangian given in Eq. (11.110), that is,

$$\begin{aligned}
\mathcal{L}_{NR_{3/2}\pi} &= -\frac{f_{NR_{3/2}\pi}}{m_\pi} \langle R^{\mu}_{3/2}| \Gamma\partial_\mu\phi_- T^{\dagger}_{+1} |N\rangle \\
&= -\frac{f_{NR_{3/2}\pi}}{m_\pi}\Gamma\partial_\mu\phi_- \begin{pmatrix} \bar{R}^{\mu++}_{3/2} & \bar{R}^{\mu+}_{3/2} & \bar{R}^{\mu0}_{3/2} & \bar{R}^{\mu-}_{3/2} \end{pmatrix} \begin{pmatrix} 1 & 0 \\ 0 & \frac{1}{\sqrt{3}} \\ 0 & 0 \\ 0 & 0 \end{pmatrix} \begin{pmatrix} p \\ n \end{pmatrix} \\
&= -\frac{f_{NR_{3/2}\pi}}{m_\pi}\Gamma\partial_\mu\phi_- (\bar{R}^{\mu++}_{3/2}\, p + \frac{1}{\sqrt{3}}\bar{R}^{\mu+}_{3/2} n). \qquad (11.111)
\end{aligned}$$

The Hermitian conjugate of this Lagrangian can be written as

$$L^{h.c.}_{NR_{\frac{3}{2}}\pi} = -\frac{f_{NR_{3/2}\pi}}{m_\pi}\Gamma\partial_\mu\phi^{\dagger}_- (\bar{p}R^{\mu++}_{3/2} + \frac{1}{\sqrt{3}}\bar{n}R^{\mu+}_{3/2}). \qquad (11.112)$$

$\Gamma = 1$ (γ_5) represents the positive (negative) parity resonances. In the following, the evaluation of the decay width considering the positive parity resonances is discussed. Using Eqs. (11.111) and (11.112) and applying Feynman rules, the transition matrix element for the decay $R^{++}_{3/2}(p_R) \to p(p) + \pi^+(k_\pi)$ as shown in Figure 11.13, is written as

$$\mathcal{M} = \frac{i f_{NR_{3/2}\pi}}{m_\pi}\bar{u}(p) k^{\mu}_{\pi} u_\mu(p_R). \qquad (11.113)$$

https://doi.org/10.1017/9781108489065.012 Published online by Cambridge University Press

The square of the transition matrix element is obtained as

$$\begin{aligned}|\mathcal{M}|^2 &= \left(\frac{f_{NR_{1/2}\pi}}{m_\pi}\right)^2 k_\pi^\mu k_\pi^\nu |\bar{u}(p)u_\mu(p_R)|^2, \\ &= \left(\frac{f_{NR_{1/2}\pi}}{m_\pi}\right)^2 k_\pi^\mu k_\pi^\nu [\mathrm{Tr}(\mathcal{P}_{\mu\nu}(p_R)(\not{p}+M)),\end{aligned} \tag{11.114}$$

where $\mathcal{P}_{\mu\nu}(p_R)$ is the projection operator for the spin $3/2$ resonances and is expressed as:

$$\mathcal{P}_{\mu\nu}(p_R) = -(\not{p}_R + M_R)\left[g_{\mu\nu} - \frac{1}{3}\gamma_\mu\gamma_\nu - \frac{2}{3}\frac{p_{R_\mu}p_{R_\nu}}{M_R^2} + \frac{1}{3}\frac{p_{R_\mu}\gamma_\nu - p_{R_\nu}\gamma_\mu}{M_R}\right]. \tag{11.115}$$

Using Eq. (11.115) in Eq. (11.114) and performing the sum over the initial spin, we obtain

$$\begin{aligned}\overline{\sum}\sum|\mathcal{M}|^2 &= \frac{2}{3}\left(\frac{f_{NR_{3/2}\pi}}{m_\pi}\right)^2\left[(p_R\cdot k_\pi)^2\left(\frac{M}{M_R}+\frac{p\cdot p_R}{M_{R^2}}\right) - m_\pi^2(p\cdot p_R + MM_R)\right], \\ &= \frac{2}{3}\left(\frac{f_{NR_{3/2}\pi}}{m_\pi}\right)^2\left[\frac{(p_R\cdot k_\pi)^2 - m_\pi^2 M_R^2}{M_R^2}\left(M_R^2 - p_R\cdot k_\pi + MM_R\right)\right],\end{aligned} \tag{11.116}$$

where we have used the momentum conservation, $p_R = p + k_\pi$. $\overline{\sum}\sum|\mathcal{M}|^2$ is evaluated in the resonance rest frame.

Using the expression of the two-body decay Γ given in Appendix E in the resonance rest frame, we obtain

$$\Gamma = \frac{|\vec{k}_\pi^{\mathrm{CM}}|}{12\pi M_R^2}\left(\frac{f_{NR_{3/2}\pi}}{m_\pi}\right)^2\left[\frac{(p_R\cdot k_\pi)^2 - m_\pi^2 M_R^2}{M_R^2}\left(M_R^2 - p_R\cdot k_\pi + MM_R\right)\right], \tag{11.117}$$

$|\vec{k}_\pi^{\mathrm{CM}}|$ represents the momentum of the outgoing pion in the resonance rest frame. Substituting $k_\pi = p_R - p$ in this expression yields the following expression for the decay width

$$\begin{aligned}\Gamma_{R_{3/2}\to N\pi} &= \frac{I_R}{12\pi M_R^2}|\vec{k}_\pi^{\mathrm{CM}}|\left(\frac{f_{NR_{3/2}\pi}}{m_\pi}\right)^2\left[\frac{(M_R^2 - M_R E_N)^2 - m_\pi^2 M_R^2}{M_R^2}\right. \\ &\times \left.\left(M_R^2 - (M_R^2 - M_R E_N) + MM_R\right)\right], \\ &= \frac{I_R}{12\pi M_R}\left(\frac{f_{NR_{3/2}\pi}}{m_\pi}\right)^2 |\vec{k}_\pi^{\mathrm{CM}}|^3 (E_N + M),\end{aligned} \tag{11.118}$$

where I_R is the isospin factor and is equal to 1 (3) for the isospin $3/2$ $(1/2)$ resonances. E_N represents the energy of the outgoing nucleon in the resonance rest frame. Similarly, the expression for the decay width of the negative parity resonances is given as

https://doi.org/10.1017/9781108489065.012 Published online by Cambridge University Press

$$\Gamma_{R_{3/2}\to N\pi} = \frac{I_R}{12\pi M_R}\left(\frac{f_{NR_{3/2}\pi}}{m_\pi}\right)^2 |\vec{k}_\pi^{\rm CM}|^3 (E_N - M). \tag{11.119}$$

The expressions for E_N and $|\vec{k}_\pi^{\rm CM}|$ are given in Eqs. (11.73) and (11.74), respectively.

11.3 Neutral Current Reactions

11.3.1 Excitation of spin $1/2$ resonances

Excitation of spin $1/2$ and isospin $1/2$ resonances

The (anti)neutrino induced neutral current (NC) production of the spin $1/2$ resonance on the nucleon target is the following:

$$\nu_l/\bar{\nu}_l\,(k) + N(p) \longrightarrow \nu_l/\bar{\nu}_l(k') + R_{1/2}(p_R). \tag{11.120}$$

The invariant matrix element for the neutral current induced process, given in Eq. (11.120) and depicted in the right panel of Figure 11.3, is written as

$$\mathcal{M} = \frac{G_F}{\sqrt{2}}\, l_\mu\, J^{\mu NC}_{\frac{1}{2}}, \tag{11.121}$$

where the leptonic current l^μ is given in Eq. (11.3). The hadronic current $J^{\mu NC}_{\frac{1}{2}}$ is defined as

$$J^{\mu NC}_{\frac{1}{2}} = \bar{u}(p_R)\Gamma^{\mu NC}_{\frac{1}{2}} u(p). \tag{11.122}$$

$\Gamma^{\mu NC}_{\frac{1}{2}}$ is the vertex function and for a positive parity resonance, $\Gamma^{\mu NC}_{\frac{1}{2}}$ is given by

$$\Gamma^{\mu NC}_{\frac{1}{2}^+} = V^{\mu NC}_{\frac{1}{2}} - A^{\mu NC}_{\frac{1}{2}}, \tag{11.123}$$

while for a negative parity resonance, $\Gamma^{\mu NC}_{\frac{1}{2}}$ is given by

$$\Gamma^{\mu NC}_{\frac{1}{2}^-} = \left[V^{\mu NC}_{\frac{1}{2}} - A^{\mu NC}_{\frac{1}{2}}\right]\gamma_5, \tag{11.124}$$

where $V^{\mu NC}_{\frac{1}{2}}$ ($A^{\mu NC}_{\frac{1}{2}}$) represents the neutral current vector (axial vector) currents and are parameterized in terms of neutral current vector and axial vector $N - R_{1/2}$ transition form factors, respectively, as,

$$V^\mu_{\frac{1}{2}} = \frac{F_1^{NC}(Q^2)}{(2M)^2}\left(Q^2\gamma^\mu + q^\mu \not{q}\right) + \frac{F_2^{NC}(Q^2)}{2M} i\sigma^{\mu\alpha}q_\alpha, \tag{11.125}$$

$$A^\mu_{\frac{1}{2}} = \left[F_A^{NC}(Q^2)\gamma^\mu + \frac{F_P^{NC}(Q^2)}{M}q^\mu\right]\gamma_5, \tag{11.126}$$

https://doi.org/10.1017/9781108489065.012 Published online by Cambridge University Press

where $F_i^{NC}(Q^2)$, $i = 1,2$ are the NC vector form factors; these form factors are, in turn, expressed in terms of the electromagnetic form factors $F_i^{R^+,R^0}(Q^2)$. $F_A^{NC}(Q^2)$ and $F_P^{NC}(Q^2)$ are the axial vector form factors for the NC induced processes. Since the contribution of the pseudoscalar form factor $F_P^{NC}(Q^2)$ is proportional to the lepton mass therefore, for NC induced processes, $F_P^{NC}(Q^2)$ vanishes. In the following sections, we determine the vector and axial vector form factors for the neutral current induced resonance production.

(i) Vector form factors

This section deals with the relation of the weak NC vector form factors $F_{1,2}^{NC}(Q^2)$ with the electromagnetic form factors $F_{1,2}^{R^+}(Q^2)$ and $F_{1,2}^{R^0}(Q^2)$ by isospin symmetry. Electromagnetic current is given in Eq. (11.13) and the vector current for the neutral current induced processes (given in Eq. (11.125)) is written as

$$V_\mu^{NC} = (1-2\sin^2\theta_W)\mathcal{V}_\mu^3 - \sin^2\theta_W\mathcal{V}_\mu^I. \tag{11.127}$$

In analogy with the charged current reactions, the transition matrix element for the $ZN \to R_{1/2}$ process is written, using Eq. (11.127), as

$$\langle R_{1/2}|\, V_\mu^{NC}\, |N\rangle = \langle R_{1/2}|\,(1-2\sin^2\theta_W)\mathcal{V}_\mu^3 - \sin^2\theta_W\mathcal{V}_\mu^I\, |N\rangle\,. \tag{11.128}$$

Using Eqs. (11.11) and (11.14) in Eq.(11.127), we obtain

$$\begin{aligned}
\langle R_{1/2}|\, V_\mu^{NC}\, |N\rangle &= \langle R_{1/2}|\,(1-2\sin^2\theta_W)V_\mu\frac{\tau_3}{2} - \sin^2\theta_W V_\mu^I I_{2\times 2}\,|N\rangle \\
&= \begin{pmatrix}\bar{R}^+_{1/2} & \bar{R}^0_{1/2}\end{pmatrix}\left[\begin{pmatrix}(1/2-\sin^2\theta_W)V_\mu & 0\\ 0 & -(1/2-\sin^2\theta_W)V_\mu\end{pmatrix}\right. \\
&- \left.\begin{pmatrix}\sin^2\theta_W V_\mu^I & 0\\ 0 & \sin^2\theta_W V_\mu^I\end{pmatrix}\right]\begin{pmatrix}p\\ n\end{pmatrix} \\
&= \bar{R}^+_{1/2}\left[\left(\frac{1}{2}-\sin^2\theta_W\right)V_\mu - \sin^2\theta_W V_\mu^I\right]p \\
&+ \bar{R}^0_{1/2}\left[-\left(\frac{1}{2}-\sin^2\theta_W\right)V_\mu - \sin^2\theta_W V_\mu^I\right]n
\end{aligned} \tag{11.129}$$

$$= V_\mu^{NC(R^+_{1/2})} + V_\mu^{NC(R^0_{1/2})}. \tag{11.130}$$

From this expression, it may be observed that the NC current consists of the components of the electromagnetic current, viz., V_μ and V_μ^I. Using Eqs. (11.21) and (11.22) in Eq. (11.129), we obtain the relation between the NC form factors $F_{1,2}^{NC}(Q^2)$ and the charged current form factors $F_{1,2}^{R^+,R^0}(Q^2)$ as

$$\begin{aligned}
F_i^{NC(R^+_{1/2})}(Q^2) &= \left(\frac{1}{2}-\sin^2\theta_W\right)(F_i^{R^+}(Q^2) - F_i^{R^0}(Q^2)) \\
&\quad - \sin^2\theta_W(F_i^{R^+}(Q^2) + F_i^{R^0}(Q^2)),
\end{aligned}$$

https://doi.org/10.1017/9781108489065.012 Published online by Cambridge University Press

$$= F_i^{R^+}(Q^2)\left(\frac{1}{2} - 2\sin^2\theta_W\right) - \frac{1}{2}F_i^{R^0}(Q^2), \quad (11.131)$$

$$F_i^{NC(R^0_{1/2})}(Q^2) = F_i^{R^0}(Q^2)\left(\frac{1}{2} - 2\sin^2\theta_W\right) - \frac{1}{2}F_i^{R^+}(Q^2). \quad (11.132)$$

(ii) Axial vector form factors

As we have seen in charged current induced processes (Eq. (11.32)), the axial vector form factor $F_A^{CC}(Q^2)$ is determined in the pion pole dominance by the application of the PCAC hypothesis. The pseudoscalar form factor $F_P^{CC}(Q^2)$ contains the pion pole. Since in neutral current induced processes, the pseudoscalar form factor $F_P^{NC}(Q^2)$ is absent, the axial vector form factor $F_A^{NC}(Q^2)$ cannot be determined by the PCAC hypothesis. In the neutral current sector, $F_A^{NC}(Q^2)$ is determined in terms of $F_A^{CC}(Q^2)$ using the isospin symmetry, where it is assumed that the axial vector current has the same structure as that of the vector current (see Eqs. (11.11) and (11.12)). With this assumption, the axial vector current for charged and neutral current induced processes is given as:

$$A_\mu^{CC} = \mathcal{A}_\mu^1 + i\mathcal{A}_\mu^2, \quad (11.133)$$

$$A_\mu^{NC} = \mathcal{A}_\mu^3. \quad (11.134)$$

Furthermore, it is assumed that $\mathcal{A}_\mu^1$, $\mathcal{A}_\mu^2$, and $\mathcal{A}_\mu^3$ form an isotriplet in the isospin space just like the vector currents. Starting with the charged current induced processes, the transition matrix element for the process $W^+n \to R^+_{1/2}$ in the case of axial vector current using Eq. (11.133) is written as

$$\begin{aligned} \langle R^+_{1/2}|\, A_\mu^{CC}\, |n\rangle &= \langle R^+_{1/2}|\, \mathcal{A}_\mu^1 + i\mathcal{A}_\mu^2\, |n\rangle\,, \\ &= \langle R^+_{1/2}|\, A_\mu \tau_+\, |n\rangle\,, \\ &= A_\mu. \end{aligned} \quad (11.135)$$

Similarly, the transition matrix element for the process $Zp \to R^+_{1/2}$ using Eq. (11.134) is written as

$$\begin{aligned} \langle R_{1/2}|\, A_\mu^{NC}\, |N\rangle &= \langle R_{1/2}|\, \mathcal{A}_\mu^3\, |N\rangle\,, \\ &= \langle R_{1/2}|\, A_\mu \frac{\tau_3}{2}\, |N\rangle\,, \\ &= \bar{R}^+_{1/2}\frac{A_\mu}{2}p + \bar{R}^0_{1/2}\frac{-A_\mu}{2}n. \end{aligned} \quad (11.136)$$

From this expression, it may be observed that A_μ connects the NC axial vector current with the CC axial vector current. From Eqs. (11.135) and (11.136), the neutral current axial vector form factor for the proton and neutron targets is given as

$$F_A^{NC(R^+_{1/2})}(Q^2) = \frac{1}{2}F_A^{CC}(Q^2), \quad (11.137)$$

$$F_A^{NC(R^0_{1/2})}(Q^2) = -\frac{1}{2}F_A^{CC}(Q^2). \quad (11.138)$$

https://doi.org/10.1017/9781108489065.012 Published online by Cambridge University Press

Excitation of spin $1/2$ and isospin $3/2$ resonances

(i) Vector form factors

Now we shall discuss the relation between the weak NC vector form factors and the electromagnetic form factors for the transition $N - R_{31}$, where the currents are purely isovector in nature. The electromagnetic current is given in Eq. (11.51) and the vector current for the weak neutral current induced processes is given as:

$$V_\mu^{NC} = (1-2\sin^2\theta_W)\mathcal{V}_\mu^3 = -(1-2\sin^2\theta_W)\sqrt{\frac{3}{2}}V_\mu T_0^\dagger. \tag{11.139}$$

Using Eq. (11.49), the transition matrix element for the neutral current induced process $ZN \to R_{1/2}^{I=3/2}$ ($R_{1/2}^{I=3/2}$ represents the spin $1/2$ and isospin $3/2$ resonances), is obtained as

$$\begin{aligned}
\langle R_{1/2}^{I=3/2}|\, V_\mu^{NC}\, |N\rangle &= -(1-2\sin^2\theta_W)\sqrt{\frac{3}{2}}\,\langle R_{1/2}^{I=3/2}|\, V_\mu T_0^\dagger\, |N\rangle\,, \\
&= -\sqrt{\frac{3}{2}}(1-2\sin^2\theta_W)\begin{pmatrix}\bar{R}_{1/2}^{++} & \bar{R}_{1/2}^{+} & \bar{R}_{1/2}^{0} & \bar{R}_{1/2}^{-}\end{pmatrix} \\
&\qquad V_\mu\begin{pmatrix} 0 & 0 \\ \sqrt{\frac{2}{3}} & 0 \\ 0 & \sqrt{\frac{2}{3}} \\ 0 & 0 \end{pmatrix}\begin{pmatrix} p \\ n\end{pmatrix} \\
&= -(1-2\sin^2\theta_W)(\bar{R}_{1/2}^{+}V_\mu p + \bar{R}_{1/2}^{0}V_\mu n).
\end{aligned} \tag{11.140}$$

From this expression, one may notice that the NC matrix elements and hence, the NC form factors for the proton and neutron induced isospin $3/2$ resonances are the same, that is,

$$F_i^{R_{1/2}^{+}}(Q^2) = F_i^{R_{1/2}^{0}}(Q^2). \tag{11.141}$$

Comparing Eqs. (11.52) and (11.140), it is found that the weak NC vector form factors $F_i^{NC(R_{1/2}^{+})}(Q^2)$ and $F_i^{NC(R_{1/2}^{0})}(Q^2)$ are related to the electromagnetic form factors $F_i^{R_{1/2}^{+}}(Q^2)$ and $F_i^{R_{1/2}^{0}}(Q^2)$, respectively, through the relation:

$$F_i^{NC(R_{1/2}^{+,0})}(Q^2) = (1-2\sin^2\theta_W)F_i^{R_{1/2}^{+,0}}(Q^2). \tag{11.142}$$

(ii) Axial vector form factors

Here, we discuss the relation between the neutral and charged current axial vector form factors for the transition $N - R_{31}$. The structure of the axial vector current is given in Eq. (11.47). Since in the isospin $1/2$ to $3/2$ transitions only the isovector current contributes, the axial vector current for the neutral current induced processes becomes

$$A_\mu^{NC} \;=\; \mathcal{A}_\mu^3 = -\sqrt{\frac{3}{2}}A_\mu T_0^\dagger, \tag{11.143}$$

https://doi.org/10.1017/9781108489065.012 Published online by Cambridge University Press

and the axial vector current for the charged current induced processes is given in Eq. (11.133). The transition matrix element for the charged current induced process $W^+N \to R_{3/2}$ is written as

$$\begin{aligned}
\langle R_{3/2}|\, A_\mu^{CC}\, |N\rangle &= \langle R_{3/2}|\, \mathcal{A}_\mu^1 + i\mathcal{A}_\mu^2\, |N\rangle = \sqrt{3}\, \langle R_{3/2}|\, A_\mu T_{+1}^\dagger\, |N\rangle \\
&= \sqrt{3}\begin{pmatrix}\bar{R}_{3/2}^{++} & \bar{R}_{3/2}^{+} & \bar{R}_{3/2}^{0} & \bar{R}_{3/2}^{-}\end{pmatrix} A_\mu \begin{pmatrix}1 & 0\\ 0 & \frac{1}{\sqrt{3}}\\ 0 & 0\\ 0 & 0\end{pmatrix}\begin{pmatrix}p\\ n\end{pmatrix} \\
&= (\sqrt{3}\bar{R}_{3/2}^{++} A_\mu p + \bar{R}_{3/2}^{+} A_\mu n).
\end{aligned} \tag{11.144}$$

This expression implies that for the $R_{3/2}^{++}$ production, the form factors should be multiplied by $\sqrt{3}$.

Similarly, for the neutral current induced processes $ZN \to R_{3/2}$, the transition matrix element is expressed as

$$\begin{aligned}
\langle R_{3/2}|\, A_\mu^{NC}\, |N\rangle &= \langle R_{3/2}|\, \mathcal{A}_\mu^3\, |N\rangle = -\sqrt{\frac{3}{2}}\, \langle R_{3/2}|\, A_\mu T_0^\dagger\, |N\rangle \\
&= -\sqrt{\frac{3}{2}}\begin{pmatrix}\bar{R}_{3/2}^{++} & \bar{R}_{3/2}^{+} & \bar{R}_{3/2}^{0} & \bar{R}_{3/2}^{-}\end{pmatrix} A_\mu \begin{pmatrix}0 & 0\\ \sqrt{\frac{2}{3}} & 0\\ 0 & \sqrt{\frac{2}{3}}\\ 0 & 0\end{pmatrix}\begin{pmatrix}p\\ n\end{pmatrix} \\
&= -(\bar{R}_{3/2}^{+} A_\mu p + \bar{R}_{3/2}^{0} A_\mu n).
\end{aligned} \tag{11.145}$$

From this equation, it can be observed that the axial vector form factors for the R_{31} resonances are the same as that in the case of proton and neutron targets, that is,

$$F_A^{NC(R_{1/2}^{+})} = F_A^{NC(R_{1/2}^{0})}. \tag{11.146}$$

Equations (11.144) and (11.145) relate the charged and neutral current axial vector form factors for R_{31} resonances by the following relation:

$$F_A^{NC}(Q^2) = -F_A^{CC}(Q^2). \tag{11.147}$$

11.3.2 Excitation of spin 3/2 resonances

Excitation of spin 3/2 and isospin 1/2 resonances

The reaction for the spin 3/2 resonance excitations induced by the neutral current on the nucleon target is written as:

$$\nu_l(\bar{\nu}_l)\ (k) + N(p) \longrightarrow \nu_l(\bar{\nu}_l)\ (k') + R_{3/2}(p_R). \tag{11.148}$$

The invariant transition amplitude for the process given in Eq. (11.148), is written as

$$\mathcal{M} = \frac{G_F}{\sqrt{2}}\, l_\mu\, J^{\mu NC}_{\frac{3}{2}}. \tag{11.149}$$

https://doi.org/10.1017/9781108489065.012 Published online by Cambridge University Press

The leptonic current l_μ is given in Eq. (11.3) and the hadronic current $J^{\mu NC}_{\frac{3}{2}}$ for the spin 3/2 resonance excitation in the neutral current sector is given as

$$J^{\mu NC}_{\frac{3}{2}} = \bar{\psi}_\nu(p')\Gamma^{\nu\mu NC}_{\frac{3}{2}} u(p), \tag{11.150}$$

where $\Gamma^{\frac{3}{2}}_{\nu\mu NC}$ has the following general structure for the positive and negative parity resonance states:

$$\Gamma^{\frac{3}{2}^+}_{\nu\mu NC} = \left[V^{\frac{3}{2}}_{\nu\mu NC} - A^{\frac{3}{2}}_{\nu\mu NC}\right]\gamma_5 \tag{11.151}$$

$$\Gamma^{\frac{3}{2}^-}_{\nu\mu NC} = V^{\frac{3}{2}}_{\nu\mu NC} - A^{\frac{3}{2}}_{\nu\mu NC}. \tag{11.152}$$

In these expressions, $V^{NC}_{\frac{3}{2}}$ ($A^{NC}_{\frac{3}{2}}$) is the vector (axial vector) current for spin 3/2 resonances for the neutral current induced processes and are given by

$$V^{\frac{3}{2}}_{\nu\mu NC} = \left[\frac{C_3^{V(NC)}}{M}(g_{\mu\nu} - q_\nu\gamma_\mu) + \frac{C_4^{V(NC)}}{M^2}(g_{\mu\nu}q\cdot p' - q_\nu p'_\mu) + \frac{C_5^{V(NC)}}{M^2}\right.$$
$$\left.(g_{\mu\nu}q\cdot p - q_\nu p_\mu) + g_{\mu\nu}C_6^{V(NC)}\right], \tag{11.153}$$

$$A^{\frac{3}{2}}_{\nu\mu NC} = -\left[\frac{C_3^{A(NC)}}{M}(g_{\mu\nu} - q_\nu\gamma_\mu) + \frac{C_4^{A(NC)}}{M^2}(g_{\mu\nu}q\cdot p' - q_\nu p'_\mu) + C_5^{A(NC)}g_{\mu\nu}\right.$$
$$\left. + \frac{C_6^{A(NC)}}{M^2}q_\nu q_\mu\right]\gamma_5, \tag{11.154}$$

where $C_i^{V(NC)}$ and $C_i^{A(NC)}$ are the vector and axial vector neutral current transition form factors. These neutral current form factors $C_i^{V(NC)}$ and $C_i^{A(NC)}$ are determined in terms of the electromagnetic form factors $C_i^{R^+,R^0}(Q^2)$ and the charged current form factors C_i^V and C_i^A using the isospin symmetry. They are discussed in the next sections.

(i) Vector form factors

In the case of the neutral current induced spin $3/2$ resonance production, the vector current is given in Eq. (11.153) with the corresponding form factors $C_i^{V(NC)}$, $i = 3,4,5,6$. $C_6^{V(NC)}(Q^2) = 0$ as required by the CVC hypothesis. As we have already discussed in earlier sections, the determination of the weak vector form factors in terms of the electromagnetic form factors depends upon the isospin of the resonance irrespective of the spin of the resonance; therefore, we directly use the expressions obtained in Subsection 11.3.1 to relate the electromagnetic and weak vector form factors. For the isospin $1/2$ and spin $3/2$ resonances, using Eqs. (11.131) and (11.132), the neutral current form factors are expressed as

$$C_i^{NC(R^+)}(Q^2) = C_i^{R^+}(Q^2)\left(\frac{1}{2} - 2\sin^2\theta_W\right) - \frac{1}{2}C_i^{R^0}(Q^2), \tag{11.155}$$

$$C_i^{NC(R^0)}(Q^2) = C_i^{R^0}(Q^2)\left(\frac{1}{2} - 2\sin^2\theta_W\right) - \frac{1}{2}C_i^{R^+}(Q^2), \tag{11.156}$$

$i = 3, 4, 5$. $C_i^{R^+}(Q^2)$ and $C_i^{R^0}(Q^2)$ are the electromagnetic form factors for the resonances R^+ and R^0, which are parameterized in terms of the helicity amplitudes $A_{1/2}$, $A_{3/2}$ and $S_{1/2}$, given in Eq. (11.84)–(11.86).

(ii) Axial vector form factors

In neutral current induced processes, the pseudoscalar form factor $C_6^{A(NC)}$ is zero due to the negligible mass of the neutrino. The axial vector form factor $C_5^{A(NC)}(Q^2)$ is determined in terms of the charged current axial vector form factor $C_5^A(Q^2)$ using the isospin symmetry which has been discussed in Subsection 11.3.1. Using Eqs. (11.137) and (11.138), the axial vector form factor for the transition $N - R_{13}$ is obtained as

$$C_5^{A(NC\ R^+_{1/2})}(Q^2) = \frac{1}{2}C_5^A(Q^2), \tag{11.157}$$

$$C_5^{A(NC\ R^0_{1/2})}(Q^2) = -\frac{1}{2}C_5^A(Q^2). \tag{11.158}$$

$C_5^A(Q^2)$ is already defined in Eq. (11.97).

1.3.2.2 Excitation of spin $3/2$ and isospin $3/2$ resonances

(i) Vector form factors

For the transition $N - R_{33}$, the vector neutral current form factors $C_i^{V(NC)}(Q^2)$, $i = 3, 4, 5$ are obtained in a similar manner as we have done for the transition $N - R_{31}$ using Eq. (11.142), and are expressed as

$$C_i^{V(NC)}(Q^2) = (1 - 2\sin^2\theta_W)C_i^V(Q^2), \qquad i = 3, 4, 5. \tag{11.159}$$

(ii) Axial vector form factors

The neutral current axial vector form factor $C_5^{A(NC)}$ for the transition $N - R_{33}$, in analogy with the neutral current axial vector form factor for the transition $N - R_{31}$, is expressed as

$$C_5^{A(NC)}(Q^2) = -C_5^A(Q^2). \tag{11.160}$$

11.4 Non-resonant Contributions

The non-resonant diagrams, shown in Figure 11.2, give the essential contribution to the single meson production through the Born diagrams in s, t, and u channels as shown in Figure 11.14.

https://doi.org/10.1017/9781108489065.012 Published online by Cambridge University Press

While the s channel diagram consist of direct nucleon poles, the t channel has meson poles and the u channel has the exchange baryon pole. Some phenomenological Lagrangians based on the pseudovector coupling or effective Lagrangians based on the chiral symmetry also include, in addition to the Born terms, the contact diagrams as shown in Figure 11.2(b).

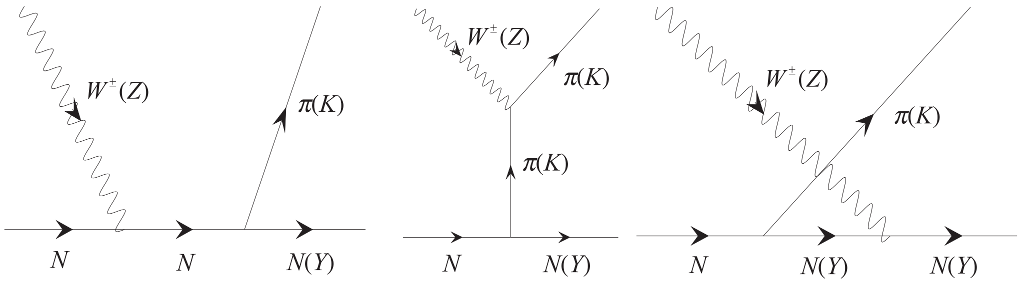

Figure 11.14 Generic Feynman diagrams for the s, t, and u channel Born terms.

In quite a general approach, the matrix element of the hadronic current is written formally as

$$\langle B(p')M(p_M)|J^\mu|N(p)\rangle = \langle B(p')M(p_M)|V^\mu + A^\mu|N(p)\rangle \quad (11.161)$$
$$= M^\mu + N^\mu, \quad (11.162)$$

where $N(p), B(p')$, and $M(p_M)$ are, respectively, the initial nucleon N of momentum p and the final baryon B of momentum p' which could be a nucleon or a hyperon and a meson π (K) of momentum p_M in case of $\Delta S = 0$ CC and NC reactions. In the case of $|\Delta S| = 1$ CC reactions, the final state has a nucleon N and a strange meson K. These particles satisfy the momentum conservation law, that is,

$$q + p = p' + p_M, \quad (11.163)$$

where $q = k - k'$ is the momentum transfer given to the hadron system, k and k' being, respectively, the momenta of the incoming neutrino and the outgoing lepton. The matrix elements M^μ and N^μ for the vector and the axial vector currents are written as

$$M^\mu = \sum_{i=1}^{8} A_i(E, E', E_\pi)\bar{u}(p')O_i^\mu(V)u(p), \quad (11.164)$$
$$N^\mu = \sum_{i=1}^{8} C_i(E, E', E_\pi)\bar{u}(p')O_i^\mu(A)u(p), \quad (11.165)$$

where $O_i^\mu(V)$ and $O_i^\mu(A)$ are eight independent covariant operators constructed from the operators γ^μ, q^μ, p^μ and k^μ, and discussed explicitly by Adler [464] and Marshak et al. [223]. The quantities $A_i(E, E', E_\pi)$ and $C_i(E, E', E_\pi)$ are the energy dependent strength of these amplitudes corresponding to the operators $O_i^\mu(V)$ and $O_i^\mu(A)$.

The gauge invariance imposed on the vector amplitudes M^μ, that is,

$$k_\mu M^\mu = 0, \quad (11.166)$$

https://doi.org/10.1017/9781108489065.012 Published online by Cambridge University Press

reduces then to six independent covariant amplitudes. The expressions for $O_i^\mu(V), i = 1-6$ and $O_i^\mu(A), i = 1-8$ are given in Table 11.10. The contribution of all the Born diagrams corresponding to the non-resonant part are explicitly calculated using a phenomenological Lagrangian for πNN interaction. The contribution of the higher resonances are calculated using the dispersion relations [460, 461, 464, 223]. Another method based on a dynamical model starting from the effective Lagrangian with bare pion–nucleon couplings obtained in the quark model, is used to construct a T matrix. Thereafter, a Lippmann–Schwinger equation is formulated and solved using coupled channel equations for pion production. In this way, it combines the effective Lagrangian with dynamical models [473, 475, 476]. In the case of effective Lagrangian approaches, the explicit contribution from individual non-resonant Born diagrams and the higher resonances are explicitly calculated in terms of the parameters describing the effective Lagrangian.

Table 11.10 Expressions for $O_i^\mu(V), i = 1-6$ and $O_i^\mu(A), i = 1-8$, where $P = p + p'$ [464].

$O_1^\mu(V)$	$\frac{1}{2}i\gamma_5[\gamma^\mu \not{q} - \not{q}\gamma^\mu]$	$O_1^\mu(A)$	$\frac{i}{2}[\not{p}_M\gamma^\mu - \gamma^\mu\not{p}_M]$
$O_2^\mu(V)$	$2i\gamma_5[P^\mu p_M \cdot q - P \cdot q p_M^\mu]$	$O_2^\mu(A)$	$2iP^\mu$
$O_3^\mu(V)$	$\gamma_5[\gamma^\mu p_M \cdot q - \not{q} p_M^\mu]$	$O_3^\mu(A)$	ip_M^μ
$O_4^\mu(V)$	$2\gamma_5[\gamma^\mu P \cdot q - \not{q} P^\mu - \frac{1}{2}iM(\gamma^\mu\not{q} - \not{q}\gamma^\mu)]$	$O_4^\mu(A)$	$-M\gamma^\mu$
$O_5^\mu(V)$	$i\gamma_5[q^\mu p_M \cdot q - q^2 p_M^\mu]$	$O_5^\mu(A)$	$-2\not{q}P^\mu$
$O_6^\mu(V)$	$\gamma_5[q^\mu\not{q} - q^2\gamma^\mu]$	$O_6^\mu(A)$	$-\not{q}p_M^\mu$
		$O_7^\mu(A)$	iq^μ
		$O_8^\mu(A)$	$-\not{q}q^\mu$

Recently, effective Lagrangians based on the chiral symmetry have been used by many authors to calculate the inelastic reactions specifically the one pion production. One class of the models [496] uses Lagrangians containing nucleon, pion, σ, ω and ρ fields consistent with chiral symmetry while another class of models is based on the non-linear sigma model incorporating chiral symmetry [481, 497, 498, 499].

In the following section, we outline the formalism to write an effective Lagrangian based on the chiral symmetry which has been used to illustrate the contributions from the non-resonant background terms given in the next chapter.

11.4.1 Chiral symmetry

The Lagrangian for QCD can be written as

$$\mathcal{L}_{\text{QCD}} = \bar{q}(i\not{D} - m_q)q - \frac{1}{4}G^\alpha_{\mu\nu}G^{\alpha\mu\nu} \tag{11.167}$$

https://doi.org/10.1017/9781108489065.012 Published online by Cambridge University Press

where $q = \begin{pmatrix} u \\ d \\ s \end{pmatrix}$ denotes the quark field and $G^{\alpha}_{\mu\nu}$ is the gluon field strength tensor with α as a color index. D_μ is defined as

$$D_\mu = \partial_\mu + ig\frac{\lambda^\alpha}{2}G_{\mu\alpha}, \tag{11.168}$$

where g is the quark–gluon coupling strength and $G_{\mu\alpha}$ is the vector gluon field. The Lagrangian written in Eq. (11.167) does not preserve chiral symmetry in its present form; however, in the limit when quark masses are assumed to be zero, the QCD Lagrangian preserves chiral symmetry. Today, it is well established that all the quarks have non-zero mass; although the current quark masses for u, d, s are small as compared to the nucleon mass. Thus, in the case of strong interactions, chiral symmetry is preserved in the limit $m_u, m_d, m_s \to 0$. The consequence of the symmetries of the Lagrangian leads to conserved currents. Vector current is conserved in nature due to isospin symmetry (Chapter 6). Similarly, the axial vector current is conserved in the presence of chiral symmetry. If the chiral symmetry is broken spontaneously, it leads to the existence of massless Goldstone bosons which are identified as pions in the limit $m_\pi \to 0$.

11.4.2 Transformation of mesons under chiral transformation

We have seen in Chapter 6 that the axial vector current is partially conserved and its consequences lead to the Goldberger–Treiman relation which relates the strong and weak couplings. The spectrum of mesons does not respect chiral symmetry. Now, we show the transformation of pion and rho mesons under the vector (Λ_V) and axial vector (Λ_A) transformations which are defined as

$$\Lambda_V\psi = e^{-i\frac{\vec{\tau}\cdot\vec{\Theta}}{2}}\psi \simeq \left(1 - i\frac{\vec{\tau}\cdot\vec{\Theta}}{2}\right)\psi, \tag{11.169}$$

$$\Lambda_A\psi = e^{-i\gamma_5\frac{\vec{\tau}\cdot\vec{\Theta}}{2}}\psi \simeq \left(1 - i\gamma_5\frac{\vec{\tau}\cdot\vec{\Theta}}{2}\right)\psi, \tag{11.170}$$

where $\psi = \begin{pmatrix} u \\ d \end{pmatrix}$ represents the quark doublet, Θ is the rotation angle, $\vec{\tau}$ represents the Pauli matrices. The pion and rho mesons can be expressed as

$$\vec{\pi} = i\bar{\psi}\vec{\tau}\gamma_5\psi, \qquad \vec{\rho}_\mu = \bar{\psi}\vec{\tau}\gamma_\mu\psi, \tag{11.171}$$

where $\vec{\pi}$, $\vec{\rho}$ represents the isovector pion and rho meson states, respectively. The subscript μ represents the vector mesons.

https://doi.org/10.1017/9781108489065.012 Published online by Cambridge University Press

The vector transformation (Eq. (11.169)) when applied on the pion state yields

$$\begin{aligned}
\pi_i &= i\bar{\psi}\tau_i\gamma_5\psi \rightarrow \Lambda_V^\dagger\bar{\psi}\tau_i\gamma_5\Lambda_V\psi, \\
&= i\bar{\psi}\left(1+\frac{i\tau_j\Theta^j}{2}\right)\tau_i\gamma_5\left(1-\frac{i\tau_j\Theta^j}{2}\right)\psi, \\
&= i\bar{\psi}\tau_i\gamma_5\psi + i\epsilon_{ijk}\Theta^j\bar{\psi}\tau_k\gamma_5\psi, \\
\vec{\pi} &\rightarrow \vec{\pi}+\vec{\Theta}\times\vec{\pi}. \qquad (11.172)
\end{aligned}$$

This expression represents the rotation of the pion state through the isospin direction by the angle Θ. Similarly, the vector transformation of the ρ mesons gives

$$\vec{\rho}_\mu \rightarrow \vec{\rho}_\mu+\vec{\Theta}\times\vec{\rho}_\mu. \qquad (11.173)$$

From Eqs. (11.172) and (11.173), it can be concluded that the vector transformation of mesons leads to rotation along the isospin direction, which means that the conservation of the vector current is associated with the isospin symmetry.

Next, we see the axial vector transformation of these meson states, starting with the pion state. For this, we start with Eq. (11.170) and obtain

$$\begin{aligned}
\pi_i &= i\bar{\psi}\tau_i\gamma_5\psi \simeq \Lambda_A^\dagger\bar{\psi}\tau_i\gamma_5\Lambda_A\psi, \\
&= i\bar{\psi}\left(1-\frac{i\gamma_5\tau_j\Theta^j}{2}\right)\tau_i\gamma_5\left(1-\frac{i\gamma_5\tau_j\Theta^j}{2}\right)\psi, \\
&= i\bar{\psi}\tau_i\gamma_5\psi + \Theta^j\bar{\psi}(\delta_{ij})\psi, \\
\Rightarrow \quad \vec{\pi} &\simeq \vec{\pi}+\vec{\Theta}\bar{\psi}\psi, \qquad (11.174) \\
&= \vec{\pi}+\vec{\Theta}\sigma, \qquad (11.175)
\end{aligned}$$

if σ is identified with the scalar particle associated with $\bar{\psi}\psi$. Eq. (11.174) represents the rotation of the pion into a linear combination of π and sigma meson when the axial vector transformation is applied on the pion state. Similarly, under axial vector transformation, a scalar meson σ $(=\bar{\psi}\psi)$ transforms as:

$$\begin{aligned}
\sigma &= \bar{\psi}\psi \simeq \Lambda_A\bar{\psi}\Lambda_A\psi, \\
&= \bar{\psi}\left(1-i\gamma_5\frac{\tau_j\Theta^j}{2}\right)\left(1-i\gamma_5\frac{\tau_j\Theta^j}{2}\right)\psi, \\
\Rightarrow \quad \sigma &\simeq \sigma-\vec{\Theta}\cdot\vec{\pi}. \qquad (11.176)
\end{aligned}$$

From Eqs. (11.174) and (11.176), it is inferred that the pion and sigma mesons under axial vector transformation, are rotated into each other.

Similarly, the transformation of the axial vector current on the ρ mesons gives

$$\begin{aligned}
\rho_{\mu_i} &\simeq \bar{\psi}\left(1-i\gamma_5\frac{\tau_j\Theta^j}{2}\right)\tau_i\gamma_\mu\left(1-i\gamma_5\frac{\tau_j\Theta^j}{2}\right)\psi, \\
\Rightarrow \quad \vec{\rho}_\mu &\simeq \vec{\rho}_\mu+\vec{\Theta}\times\vec{a}_{1_\mu}, \qquad (11.177)
\end{aligned}$$

https://doi.org/10.1017/9781108489065.012 Published online by Cambridge University Press

where $\vec{a}_{1_\mu} = \bar{\psi}\vec{\tau}\gamma_\mu\gamma_5\psi$ represents a vector meson a_1 with spin 1. The axial vector transformation of rho mesons shows the existence of a_1 mesons. Moreover, the two, that is, rho and a_1 mesons are rotated into one another by the axial vector transformation.

Therefore, if the chiral symmetry is good, then $(\pi,\ \sigma)$ and $(\rho,\ a_1)$ should be degenerate, which is not true experimentally. This is because we know that σ is not observed experimentally. In the case of ρ and a_1 meson states, the mass of ρ is $m_\rho = 0.77$ GeV while the mass of a_1 is $m_{a_1} = 1.23 \pm 0.04$ GeV. Since there is a large mass difference between the masses of ρ and a_1, the chiral symmetry is broken in nature at the nucleon level. However, if the chiral symmetry is broken spontaneously, then the degeneracy of states is not a required consequence (Chapter 7). Moreover, in this case, massless Goldstone bosons appear which are identified as pions. A small mass of pions can be generated by assigning a non-zero but very small mass to the fermions in the theory which leads to an axial vector current consistent with PCAC [500, 163]. Thus the degeneracy of mass spectrum is not present in the case of spontaneous breaking of the symmetry, which generates pion mass and leads to PCAC.

11.4.3 Linear sigma model

The linear sigma model is an effective chiral model introduced by Gell-Mann and Levy in 1960 to study the chiral symmetry in the pion–nucleon system before the formulation of QCD. Spontaneous symmetry breaking and PCAC are the natural consequences of this model. The structure of the Lagrangian is Lorentz scalar; it is also invariant under vector (Λ_V) and axial vector (Λ_A) transformations. We have studied in the earlier sections that the pion as well as sigma fields are not invariant under axial vector transformations. Our task is to first construct a field variable which is invariant under both Λ_V and Λ_A and then write the Lagrangian using it.

We have discussed in Section 11.4.2 that the vector transformation is nothing but the isospin rotation; thus, the squares of these fields are also invariant under vector transformation:

$$\pi^2 \xrightarrow{\Lambda_V} \pi^2 \qquad\qquad \sigma^2 \xrightarrow{\Lambda_V} \sigma^2, \tag{11.178}$$

while under the axial vector transformation, even the square of the meson fields are not invariant and yields the following expressions in the limit of small $\vec{\Theta}$:

$$\pi^2 \xrightarrow{\Lambda_A} \pi^2 + 2\sigma\vec{\Theta}\cdot\vec{\pi} \qquad\qquad \sigma^2 \xrightarrow{\Lambda_A} \sigma^2 - 2\sigma\vec{\Theta}\cdot\vec{\pi}. \tag{11.179}$$

Furthermore, from Eqs. (11.178) and (11.179), one may notice that the combination $\sigma^2 + \pi^2$ is invariant under both vector and axial vector transformations. This combination is also Lorentz invariant; hence, the Lagrangian for the linear sigma model can be constructed around $\sigma^2 + \pi^2$.

The most general Lagrangian of the linear sigma model for the pion–nucleon interaction is written as [501, 502]:

$$\begin{aligned}\mathcal{L}_{LSM} &= i\bar{\psi}\partial_\mu\gamma^\mu\psi + \frac{1}{2}\partial_\mu\pi\partial^\mu\pi + \frac{1}{2}\partial_\mu\sigma\partial^\mu\sigma \\ &- g_\pi(i\bar{\psi}\gamma_5\vec{\tau}\psi\vec{\pi} + \bar{\psi}\psi\sigma) - \frac{\lambda}{4}\left((\pi^2+\sigma^2) - f_\pi^2\right)^2,\end{aligned} \tag{11.180}$$

https://doi.org/10.1017/9781108489065.012 Published online by Cambridge University Press

where ψ, π, and σ represent the nucleon, pion, and sigma fields, respectively, g_π is the pion–nucleon coupling, and f_π represents the pion decay constant. The first term in Eq. (11.180) represents the kinetic energy of the nucleon, which is the Lagrangian of the massless nucleons. The second and third terms represent the kinetic energy of the pion and sigma mesons. The fourth term represents the pion–nucleon interaction term which is generally expressed by the term $g_\pi(i\bar{\psi}\gamma_5\vec{\tau}\psi)\vec{\pi}$ and transforms like π^2 under Λ_V and Λ_A transformations, while π^2 is not invariant under Λ_A transformation and one requires a term which transforms like σ^2 to make the potential chiral invariant. The simplest choice for a Lagrangian which transforms like σ^2 is $g_\pi\bar{\psi}\psi\sigma$; thus, sigma is incorporated in the pion–nucleon potential to make it chiral invariant. The last term in Eq. (11.180) represents the pion sigma potential. The vacuum expectation value of σ is generated by this potential; thus, the chiral invariance requires that the potential must be a function of $\pi^2 + \sigma^2$. The simplest form of this potential is given by the last term in the aforementioned Lagrangian, where f_π represents the minimum of this potential.

In the Lagrangian given in Eq. (11.180), all the interaction terms between pion, nucleon, and sigma are present except the mass terms. The mass term for the nucleon is generated without breaking the chiral symmetry, by its interaction with the sigma field which is given by the potential $g_\pi(\bar{\psi}\psi)\sigma$. This is achieved by giving a finite vacuum expectation value to the sigma fields

$$< \sigma >= \sigma_0, \tag{11.181}$$

which describes the spontaneous breaking of the chiral symmetry. By this mechanism, the nucleon mass is generated. Due to the spontaneously broken chiral symmetry, the pion remains massless and sigma obtains a mass term through its coupling with the vacuum expectation value of the sigma field from the last terms in Eq. (11.180). Thus, in the linear sigma model, the pion is massless but sigma is massive.

11.4.4 Explicitly broken chiral symmetry

The chiral symmetry is a good symmetry in the limit of vanishing quark masses. In the presence of the quark mass terms in the Lagrangian, although being very small for the lowest lying u, d, s quarks, the chiral symmetry is broken explicitly.

One can visualize the effect of the explicit symmetry breaking as shown in Figure 11.15. In the case of explicit symmetry breaking, the Hamiltonian and in turn, the potential is not symmetric under rotation. The ground state of the potential is shifted but the shift is so small that the rotation along the pion axis and the radial excitation along the σ-axis in the case of spontaneous breaking of the chiral symmetry remains almost undisturbed. Spontaneous and explicit symmetry breaking generate, respectively, nucleon and pion masses. Thus, in the limit of the small explicit breaking, the effect of the spontaneous breaking of the chiral symmetry still dominates the effect of the explicit breaking. This means that the chiral symmetry is good even in the limit of the small explicit symmetry breaking effect. The effect of the explicit symmetry breaking on the linear sigma model makes the pions massive. However, the problem lies with the massive σ field as the σ meson has not been observed experimentally. Therefore, a non-linear sigma model was proposed which is discussed in the next section [501].

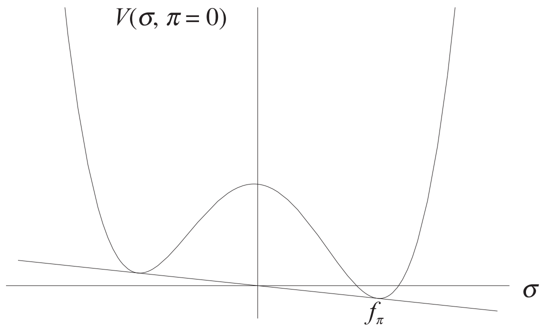

Figure 11.15 Effect of explicit symmetry breaking.

11.4.5 Non-linear sigma model

In the non-linear sigma model, this massive σ field is removed by taking an infinitely large coupling λ which results in an infinite mass of the σ meson; the potential gets infinitely steep in the sigma direction as depicted in Figure 11.16. The minimum of this potential defines a circle (known in the literature as the chiral circle but, in principle, it is a sphere not a circle) described by

$$\pi^2 + \sigma^2 = f_\pi^2. \tag{11.182}$$

The dynamics of the system is confined to the rotation along this circle. Thus, the pion and sigma meson fields can be expressed in terms of the pion fields $\vec{\Phi}(x)$ and the radius of the circle f_π, as

$$\sigma(x) = f_\pi \cos\left(\frac{\Phi(x)}{f_\pi}\right), \tag{11.183}$$

$$\vec{\pi}(x) = f_\pi \hat{\Phi} \sin\left(\frac{\Phi(x)}{f_\pi}\right), \tag{11.184}$$

where $\Phi = \sqrt{\vec{\Phi} \cdot \vec{\Phi}}$ and $\hat{\Phi} = \frac{\vec{\Phi}}{\Phi}$.

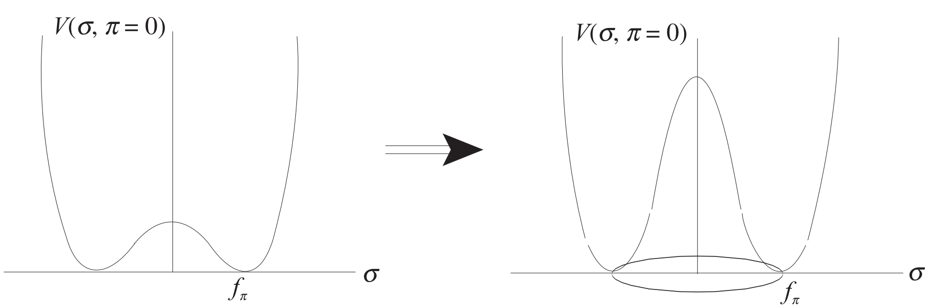

Figure 11.16 Figure depicting the infinitely steep potential in the σ direction.

https://doi.org/10.1017/9781108489065.012 Published online by Cambridge University Press

The pion and sigma fields can be expressed in the complex form as

$$U(x) = e^{\frac{i\vec{\tau}\cdot\vec{\Phi}(x)}{f_\pi}} = \cos\left(\frac{\Phi(x)}{f_\pi}\right) + i\vec{\tau}\hat{\Phi}\sin\left(\frac{\Phi(x)}{f_\pi}\right) = \frac{1}{f_\pi}(\sigma + i\vec{\tau}\cdot\vec{\pi}), \tag{11.185}$$

where $U(x)$ is the unitary 2×2 matrix. In terms of the complex field, the chiral circle is expressed as

$$\frac{1}{2}\mathrm{Tr}(U^\dagger U) = \frac{1}{f_\pi}(\sigma^2 + \pi^2) = 1. \tag{11.186}$$

As in the case of the vector current, isospin symmetry corresponds to the rotational symmetry; analogously, the chiral symmetry corresponds to the rotational symmetry along the chiral circle.

The Lagrangian for the linear sigma model given in Eq. (11.180) is now expressed in terms of Φ or the complex representation $U(x)$.

Writing the kinetic energy terms of the mesons in terms of $U(x)$, we get

$$\frac{1}{2}(\partial_\mu\sigma\partial^\mu\sigma + \partial_\mu\vec{\pi}\partial^\mu\vec{\pi}) = \frac{f_\pi^2}{4}(\partial_\mu U^\dagger\partial^\mu U). \tag{11.187}$$

Similarly, the nucleon–meson coupling term modifies as

$$\begin{aligned}
-g_\pi(\bar{\psi}\psi\sigma + i\bar{\psi}\gamma_5\vec{\tau}\psi\vec{\pi}) &= -g_\pi\bar{\psi}\left(f_\pi\cos\left(\frac{\Phi}{f_\pi}\right) + i\gamma_5\vec{\tau}f_\pi\hat{\Phi}\sin\left(\frac{\Phi}{f_\pi}\right)\right)\psi,\\
&= g_\pi f_\pi\bar{\psi}e^{\frac{i\gamma_5\vec{\tau}.\vec{\Phi}}{f_\pi}}\psi,\\
&= g_\pi f_\pi\bar{\psi}\Lambda\Lambda\psi,
\end{aligned} \tag{11.188}$$

with $\Lambda = e^{\frac{i\gamma_5\vec{\tau}.\vec{\Phi}}{2f_\pi}}$.

Redefining the nucleon field ψ in terms of ψ_W as

$$\psi_W = \Lambda\psi, \tag{11.189}$$

the nucleon–meson interaction becomes

$$-g_\pi(\bar{\psi}\psi\sigma + i\bar{\psi}\gamma_5\vec{\tau}\psi\vec{\pi}) = -g_\pi f_\pi\bar{\psi}_W\psi_W = -M\bar{\psi}_W\psi_W, \tag{11.190}$$

where the Goldberger–Treiman relation ($g_\pi = \frac{g_{\pi NN}}{\sqrt{2}}$; $g_\pi f_\pi = M$) is used. Thus, in the non-linear sigma model, the nucleon–meson interaction term reduces to the nucleon mass term. In terms of the redefined nucleon field ψ_W, the nucleon kinetic energy term is modified as:

$$\begin{aligned}
\bar{\psi}(i\partial\!\!\!/)\psi &= \bar{\psi}_W\Lambda^\dagger(i\partial^\mu\gamma_\mu)\Lambda^\dagger\psi_W,\\
&= \bar{\psi}_W(i\partial\!\!\!/ + \gamma_\mu V^\mu + \gamma_\mu\gamma_5 A^\mu)\psi_W,
\end{aligned} \tag{11.191}$$

https://doi.org/10.1017/9781108489065.012 Published online by Cambridge University Press

where V^μ and A^μ are defined in terms of the unitary matrix u as

$$V^\mu = \frac{1}{2}[u^\dagger \partial^\mu u + u\partial^\mu u^\dagger], \tag{11.192}$$

$$A^\mu = \frac{i}{2}[u^\dagger \partial^\mu u - u\partial^\mu u^\dagger], \tag{11.193}$$

and

$$u = e^{\frac{i\vec{\tau}.\vec{\Phi}}{2f_\pi}}; \quad U = u^2. \tag{11.194}$$

The last term of the Lagrangian given in Eq. (11.180) vanishes as the potential between the pion and sigma fields vanishes in the chiral limit ($\pi^2 + \sigma^2 = f_\pi^2$). Thus, the Lagrangian for the non-linear sigma model in the chiral limit becomes

$$\mathcal{L}_{NLSM} = \bar{\psi}_W(i\partial\!\!\!/ + \gamma_\mu V^\mu + \gamma_\mu\gamma_5 A^\mu - M)\psi_W + \frac{f_\pi^2}{4}(\partial_\mu U^\dagger \partial^\mu U), \tag{11.195}$$

where the first term of this Lagrangian represents the interaction between the nucleons and pions (in general, between baryons and mesons) and the second term represents the interaction between pions (in general, mesons). The Lagrangian in Eq. (11.195) can be expanded in terms of the single variable, $\vec{\Phi}(x)$, which represents the pion field. Noticeably, the sigma field which was present in the linear sigma model disappeared in the Lagrangian for the non-linear sigma model. An important point to keep in mind regarding the Lagrangian given in Eq. (11.195) is that it represents only the interaction between pions and nucleons but not the interaction of these particles with the gauge bosons.

In reality, all the interactions proceed via the exchange of gauge bosons. Thus, our next task is to incorporate the gauge bosons in the meson–meson and meson–baryon Lagrangians which can be discussed in the next section. It is also worth mentioning that the unitary matrix U is expressed in terms of the Pauli matrices $\vec{\tau}$ representing the SU(2) isospin symmetry; however, one may extend the Lagrangian given in Eq. (11.195) to the SU(3) isospin symmetry, that is, through the inclusion of the octet of mesons and baryons.

11.4.6 Lagrangian for the meson–meson and meson–gauge boson interactions

The Lagrangian for the meson–meson interaction is given in Eq. (11.195) (second term), where in the unitary matrix $U = e^{\frac{i\vec{\tau}\vec{\Phi}(x)}{f_\pi}}$, $\vec{\tau}$ stands for the SU(2) isospin symmetry. In order to extend the meson–meson Lagrangian for the SU(3) symmetry (where the three massless quarks; u, d, s are considered), the Lagrangian remains the same; the only change is the modification of U, which in the SU(3) symmetry becomes

$$U(x) = e^{\frac{i\vec{\lambda}\cdot\vec{\Phi}(x)}{f_\pi}} = e^{\frac{i\lambda_i\Phi_i(x)}{f_\pi}}; \qquad i = 1-8, \tag{11.196}$$

https://doi.org/10.1017/9781108489065.012 Published online by Cambridge University Press

where λ represents the Gell-Mann matrices which are given in Appendix B and Φ_i represents the octet of the meson fields, expressed as

$$\vec{\lambda}\cdot\vec{\Phi} = \sum_{i=1}^{8}\lambda_i\Phi_i = \begin{pmatrix} \Phi_3+\frac{1}{\sqrt{3}}\Phi_8 & \Phi_1-i\Phi_2 & \Phi_4-i\Phi_5 \\ \Phi_1+i\Phi_2 & -\Phi_3+\frac{1}{\sqrt{3}}\Phi_8 & \Phi_6-i\Phi_7 \\ \Phi_4+i\Phi_5 & \Phi_6+i\Phi_7 & -\frac{2}{\sqrt{3}}\Phi_8 \end{pmatrix}$$
$$= \begin{pmatrix} \pi^0+\frac{1}{\sqrt{3}}\eta & \sqrt{2}\pi^+ & \sqrt{2}K^+ \\ \sqrt{2}\pi^- & -\pi^0+\frac{1}{\sqrt{3}}\eta & \sqrt{2}K^0 \\ \sqrt{2}K^- & \sqrt{2}\bar{K}^0 & -\frac{2}{\sqrt{3}}\eta \end{pmatrix}. \quad (11.197)$$

With these modifications, the second term of the Lagrangian given in Eq. (11.195) gives the interaction among the octets of the pseudoscalar mesons. Using Eqs. (11.196) and (11.197) in the second term of the Lagrangian given in Eq. (11.195), one obtains the Lagrangians for different meson–meson interactions. Here, for the sake of completeness, we write down the Lagrangians for the $\pi^+\pi^+ \to \pi^+\pi^+$ and $\pi^+\pi^- \to K^+K^-$ interactions,

$$\mathcal{L}_{\pi\pi\pi\pi} = \frac{\pi^+\partial_\mu\pi^-\pi^+\partial^\mu\pi^-}{2f_\pi^2}, \quad (11.198)$$
$$\mathcal{L}_{\pi\pi KK} = \frac{\pi^+\pi^-\partial_\mu K^-\partial^\mu K^+}{2f_\pi^2}. \quad (11.199)$$

However, in the real world (as we will see in the next chapter), we need the interaction of these mesons with the gauge bosons. The gauge boson fields are incorporated in the meson–meson Lagrangian by replacing the partial derivative ∂_μ with the covariant derivative D_μ, that is,

$$\mathcal{L}_{MM} = \frac{f_\pi^2}{4}(D_\mu U^\dagger D^\mu U), \quad (11.200)$$

where $D_\mu U$ and $D_\mu U^\dagger$ is written as

$$D_\mu U = \partial_\mu U - ir_\mu U + iUl_\mu, \quad (11.201)$$
$$D_\mu U^\dagger = \partial_\mu U^\dagger + iU^\dagger r_\mu - il_\mu U^\dagger. \quad (11.202)$$

r_μ and l_μ, respectively, represents the right- and left-handed currents, defined in terms of the vector (v_μ) and axial vector (a_μ) fields as

$$l_\mu = \frac{1}{2}(v_\mu - a_\mu), \qquad r_\mu = \frac{1}{2}(v_\mu + a_\mu). \quad (11.203)$$

The vector and axial vector fields are different for the interaction of the different gauge bosons with the meson fields. In the following, we explicitly discuss the interaction of the photon, $W^\pm$ and Z^0 with the meson–meson Lagrangian for the electromagnetic, charged current and neutral current induced processes, respectively.

Interaction with the photon field

Since we know that the electromagnetic interactions are purely vector in nature, the axial vector current does not contribute; thus, the left- and right-handed currents are identical and are expressed as

$$l_\mu = r_\mu = -e\hat{Q}A_\mu, \tag{11.204}$$

where e is the electric charge, A_μ represents the photon field, and $\hat{Q} = \begin{pmatrix} 2/3 & 0 & 0 \\ 0 & -1/3 & 0 \\ 0 & 0 & -1/3 \end{pmatrix}$ represents the charge of $u,\ d,\ s$ quarks.

Using Eqs. (11.204), (11.201), and (11.202) in Eq. (11.200), one obtains the Lagrangian for the mesons interacting with the photons. For example, here we write the Lagrangians for the $\gamma\pi^+ \to \pi^+$ and $\pi^+\pi^- \to \gamma\gamma$ processes, as

$$\mathcal{L}_{\gamma\pi\pi} = -ie\pi^+\partial_\mu\pi^- A^\mu, \tag{11.205}$$
$$\mathcal{L}_{\gamma\gamma\pi\pi} = -e^2\pi^+\pi^- A_\mu A^\mu. \tag{11.206}$$

Lagrangians for the different interactions are obtained in a similar manner.

Interaction with $W^\pm$ field

In the case of weak charged and neutral current induced processes, both vector and axial vector fields contribute; thus, the left- and right-handed currents are expressed as

$$l_\mu = -\frac{g}{2}(W_\mu^+ T_+ + W_\mu^- T_-), \qquad r_\mu = 0, \tag{11.207}$$

where $g = \frac{e}{\sin\theta_W}$, θ_W is the Weinberg angle, $W_\mu^\pm$ represents the W boson field and $T_\pm$ is defined as

$$T_+ = \begin{pmatrix} 0 & V_{ud} & V_{us} \\ 0 & 0 & 0 \\ 0 & 0 & 0 \end{pmatrix}, \qquad \text{and} \qquad T_- = \begin{pmatrix} 0 & 0 & 0 \\ V_{ud} & 0 & 0 \\ V_{us} & 0 & 0 \end{pmatrix}, \tag{11.208}$$

with $V_{ud} = \cos\theta_C$ and $V_{us} = \sin\theta_C$ being the elements of the Cabibbo–Kobayashi–Maskawa matrix and θ_C being the Cabibbo angle.

Using Eqs. (11.207), (11.201), and (11.202) in Eq. (11.200), the Lagrangian for the interaction of mesons with W bosons is written. The Lagrangians for $W^+\pi^0 \to \pi^+$ and $W \to \pi$ processes are written as:

$$\mathcal{L}_{W\pi\pi} = \frac{ig}{2}V_{ud}\pi^-\partial_\mu\pi^0 W^{+\mu}, \tag{11.209}$$
$$\mathcal{L}_{W\pi} = -\frac{g}{2}f_\pi V_{ud}\partial_\mu\pi^- W^{+\mu}. \tag{11.210}$$

https://doi.org/10.1017/9781108489065.012 Published online by Cambridge University Press

Interaction with Z^0 field

The left- and right-handed currents for the neutral current induced processes are expressed as

$$l_\mu = \left(-\frac{g}{\cos\theta_W} + e\tan\theta_W\right) Z_\mu \frac{\lambda_3}{2}, \qquad r_\mu = g\tan\theta_W \sin\theta_W Z_\mu \frac{\lambda_3}{2}, \quad (11.211)$$

where Z_μ represents the Z boson field and λ_3 is the third component of the Gell-Mann matrices.

Using Eqs. (11.211), (11.201), and (11.202) in Eq. (11.200), the Lagrangian for the interactions of the Z boson with the meson field is obtained. The Lagrangians for the $Z\pi \to \pi$ and $Z \to \pi$ processes are written as:

$$\mathcal{L}_{Z\pi\pi} = \frac{ig}{2\cos\theta_W}(1 - 2\sin^2\theta_W)\pi^+\partial_\mu\pi^- Z^\mu, \quad (11.212)$$

$$\mathcal{L}_{Z\pi} = -\frac{g}{2\cos\theta_W} f_\pi \partial_\mu \pi^0 Z^\mu. \quad (11.213)$$

11.4.7 Lagrangian for the meson–baryon–gauge boson interaction

The Lagrangian for the meson–baryon interaction is given as the first term of Eq. (11.195), where V_μ and A_μ are defined in terms of a unitary matrix u given in Eq. (11.194) for the SU(2) symmetry. The modification of u by the following expression:

$$u(x) = e^{\frac{i\vec{\Phi}\cdot\vec{\lambda}}{2f\pi}}, \quad (11.214)$$

leads to the meson–baryon Lagrangian in the SU(3) symmetry. The Lagrangian for the meson–baryon interaction can be rewritten as

$$\mathcal{L}_{MB} = \mathrm{Tr}[\bar{B}(i\not{D} - M)B] - \frac{D}{2}\mathrm{Tr}[\bar{B}\gamma_\mu\gamma_5\{u^\mu, B\}] - \frac{F}{2}\mathrm{Tr}[\bar{B}\gamma_\mu\gamma_5[u^\mu, B]], \quad (11.215)$$

where M represents the baryon mass. D and F are the axial vector coupling constants for the baryon octet obtained from the analysis of the semileptonic decays of neutron and hyperons. B represents the baryon field, defined as

$$B(x) = \sum_{i=1}^{8} \frac{1}{\sqrt{2}} b_i\lambda_i = \frac{1}{\sqrt{2}}\begin{pmatrix} b_3 + \frac{1}{\sqrt{3}}b_8 & b_1 - ib_2 & b_4 - ib_5 \\ b_1 + ib_2 & -b_3 + \frac{1}{\sqrt{3}}b_8 & b_6 - ib_7 \\ b_4 + ib_5 & b_6 + ib_7 & -\frac{2}{\sqrt{3}}b_8 \end{pmatrix}$$
$$= \begin{pmatrix} \frac{1}{\sqrt{2}}\Sigma^0 + \frac{1}{\sqrt{6}}\Lambda & \Sigma^+ & p \\ \Sigma^- & -\frac{1}{\sqrt{2}}\Sigma^0 + \frac{1}{\sqrt{6}}\Lambda & n \\ \Xi^- & \Xi^0 & -\frac{2}{\sqrt{6}}\Lambda \end{pmatrix}, \quad (11.216)$$

with b_i being the component of the baryon field. The quantities $D_\mu B$ and u^μ are defined as

$$D_\mu B = \partial_\mu B + [\Gamma_\mu, B], \quad (11.217)$$

$$u^\mu = i[u^\dagger(\partial^\mu - ir^\mu)u - u(\partial^\mu - il^\mu)u^\dagger], \quad (11.218)$$

https://doi.org/10.1017/9781108489065.012 Published online by Cambridge University Press

with

$$\Gamma_\mu = \frac{1}{2}[u^\dagger(\partial^\mu - ir^\mu)u - u(\partial^\mu - il^\mu)u^\dagger]. \tag{11.219}$$

u is defined in Eq. (11.194). r_μ and l_μ, respectively, represents the right- and left-handed currents, defined in terms of the vector (v_μ) and axial vector (a_μ) fields and are given in Eq. (11.203). These currents represent the interaction of the gauge bosons with the meson–baryon Lagrangian. Thus, the vector and axial vector fields are different for the interaction of the different gauge bosons. In the following sections, we present the Lagrangians for the interaction of the photon, $W^\pm$, and Z^0 bosons with the mesons and baryons for the electromagnetic, charged current, and neutral current induced processes, respectively.

Interaction with the photon field

The left- and right-handed currents are given in Eq. (11.204) using Eqs. (11.204) and (11.216)–(11.219) in Eq. (11.215). The Lagrangian for the interaction of mesons and baryons among themselves and with the photon (γ) fields is obtained. For example, here we write the Lagrangians for the $\gamma p \to p$, $p \to p\pi^0$ and $\gamma p \to n\pi^+$ processes, as

$$\mathcal{L}_{\gamma pp} = -e\,\bar{p}\gamma_\mu p\,A^\mu, \tag{11.220}$$

$$\mathcal{L}_{pp\pi^0} = -\frac{(D+F)}{2f_\pi}\bar{p}\gamma_\mu\gamma_5 p\,\partial^\mu\pi^0, \tag{11.221}$$

$$\mathcal{L}_{\gamma pn\pi^+} = \frac{ie}{\sqrt{2}f_\pi}(D+F)\,\bar{n}\gamma_\mu\gamma_5 p\,A^\mu\pi^-. \tag{11.222}$$

In a similar manner, one may obtain the Lagrangians for the different possible interactions of the meson–baryon system with the photon field.

Interaction with $W^\pm$ field

In the case of weak charged current induced processes, the left- and right-handed currents are expressed as in Eq. (11.207). Using Eqs. (11.207) and (11.216)–(11.219) in Eq. (11.215), the Lagrangian for the interaction of the W bosons with the meson–baryon system is obtained. The Lagrangians for the processes $W^+n \to p$ and $W^+n \to p\pi^0$ are written as:

$$\mathcal{L}_{Wnp} = -\frac{g}{2\sqrt{2}}V_{ud}\,\bar{p}[\gamma_\mu - (D+F)\gamma_\mu\gamma_5]n\,W^{+\mu}, \tag{11.223}$$

$$\mathcal{L}_{Wnp\pi^0} = -\frac{ig}{2\sqrt{2}f_\pi}V_{ud}\,\bar{p}[\gamma_\mu - (D+F)\gamma_\mu\gamma_5]n\,W^{+\mu}. \tag{11.224}$$

Interaction with Z^0 field

The expressions for the left- and right-handed currents in the case of neutral current induced processes are given in Eq. (11.211). The Lagrangian for the interactions of the Z-boson with the meson–baryon system is obtained using Eqs. (11.211) and (11.216)–(11.219) in Eq. (11.215).

https://doi.org/10.1017/9781108489065.012 Published online by Cambridge University Press

The Lagrangians for the interactions $Zp \to p$ and $Zp \to n\pi^+$ processes are written as:

$$\mathcal{L}_{Zpp} = -\frac{g}{4\cos\theta_W}\,\bar{p}[\gamma_\mu(1-2\sin^2\theta_W)-(D+F)\gamma_\mu\gamma_5]p\,Z^\mu, \tag{11.225}$$

$$\mathcal{L}_{Zpn\pi^+} = \frac{ig}{2\sqrt{2}f_\pi\cos\theta_W}\,\bar{p}[\gamma_\mu-(1-2\sin^2\theta_W)(D+F)\gamma_\mu\gamma_5]n\,\pi^+Z^\mu. \tag{11.226}$$

The Lagrangians which we have discussed in this chapter are used to write the matrix element for specific processes. The matrix element for the different processes and the differential scattering cross sections are obtained in the next chapter.